Sedimentary Geology 317 (2015) 9–26

Contents lists available at ScienceDirect

Sedimentary Geology

journal homepage: www.elsevier.com/locate/sedgeo

Origin and architecture of a Mass Transport Complex on the northwest slope of Little Bahama Bank (Bahamas): Relations between off-bank transport, bottom current sedimentation and submarine landslides

E. Tournadour [a,b,*], T. Mulder [a], J. Borgomano [b], V. Hanquiez [a], E. Ducassou [a], H. Gillet [a]

[a] Université de Bordeaux, UMR 5805 EPOC, Allée Geoffroy St Hilaire, 33615 Pessac cedex, France
[b] TOTAL, CSTJF, Avenue Larribau, 64018 Pau cedex, France

ARTICLE INFO

Article history:
Received 22 February 2014
Received in revised form 29 September 2014
Accepted 8 October 2014
Available online 16 October 2014

Keywords:
Carbonate slope systems
Bahamas
Mass Transport Complex (MTC)
Contourite drift
Off-bank transport sedimentation

ABSTRACT

The analysis of the sedimentary dynamics of the carbonate slope of the northwest part of Little Bahama Bank (LBB, Bahamas) reveals a complex interaction between slope destabilisations, off-bank sediment export and longitudinal transport, the latter being driven by the Antilles and the Florida currents, at the northern end of the Florida Strait. Their combined action since the middle Miocene resulted in an extensional growth slope, previously called 'LBB Drift' (Mullins et al., 1980). Deposition within this extensional growth slope is dominated by either platform-derived downslope sedimentation or bottom current sedimentation. The latter induces the formation of a plastered drift, showing both upslope and downslope migrations, which do not correspond to the 'LBB Drift' as described by Mullins et al. (1980). Interestingly, a large submarine landslide affects the upper part of this plastered drift, and displays a complex and striking geomorphology on the seafloor. A new high-quality multibeam echosounder and seismic dataset allowed a detailed characterisation of the architecture of this Mass Transport Complex (MTC). A 44 km-long circular incision at 275 m and 460 m water depths, with a steep external edge (from 40 to 70 m high), forms the only present day evidence of this ancient MTC. It comprises confined Mass Transport Deposits (MTDs), which are delimited by frontal and lateral edges that developed inside the plastered drift. The top of this plastered drift is marked by a major erosional surface, most likely induced by an increase in oceanic current circulation. Channelised geometries, laterally associated with overspill deposits, developed within the depression induced by the MTC, and are an additional evidence of bottom current activity in this area. In addition, recent pockmarks are visible on the seafloor in front of the circular scarp of the MTC and probably relate to fluid escape, originating from the underlying MTDs' compressional area.

All these features seen on the northwest slope of LBB bring new understanding on MTC sedimentary processes and associated morphologies in carbonate slope settings. Furthermore, this study highlights the interplay between off-bank transport, oceanic circulation and mass flow processes, which are seen as key processes in the shaping of Bahamian slopes and in their sedimentary dynamics.

1. Introduction

During the last decades, both academic and industrial studies of turbidite systems have been mostly focused on siliciclastic systems, neglecting carbonate gravity systems as they are often considered to have a poor reservoir and hydrocarbon potential. Carbonate turbidite systems differ from the frequent point-source siliciclastic systems because of their linear sediment input source, which predominantly depends on the carbonate production on the platform, whereas siliciclastic systems are usually controlled by continental relief erosion and river discharge (Mullins and Cook, 1986; Mullins et al., 1984). Hitherto, several studies on ancient systems (*e.g.* Betzler et al., 1999; Borgomano, 2000; Eberli et al., 1997; Janson et al., 2011; Phelps and Kerans, 2007; Playton et al., 2010; Savary and Ferry, 2004; Vecsei and Sanders, 1997) revealed some general features of resedimentation systems on carbonate slopes. However, detailed morphologies, architecture, sedimentary processes and controlling parameters of resedimented carbonates remain poorly documented and understood. Improving our knowledge of these systems implies the study of modern carbonate slopes, such as the Bahamian slopes. This present-day analog offers the opportunity to characterise sedimentation processes across a continuous platform to basin transect during the Quaternary. In addition, the Bahamas are one of the best-studied modern carbonate systems (Bergman et al., 2010) and hence provide a solid framework regarding their overall geological setting and knowledge on sedimentation processes.

* Corresponding author at: Université de Bordeaux, UMR 5805 EPOC, Allée Geoffroy St Hilaire, 33615 Pessac cedex, France. Tel.: +33 5 40 00 84 38.
E-mail address: e.tournadour@epoc.u-bordeaux.fr (E. Tournadour).

http://dx.doi.org/10.1016/j.sedgeo.2014.10.003
0037-0738/

Bahamian slope environments are influenced by three major controlling factors: (1) sediment transport from the platform which is directly related to carbonate production. Deep sediments of the Bahamas show a mixture of pelagic and platform-derived materiel called 'periplatform ooze' (Schlager and James, 1978). The input of platform-derived material is thought to be higher during highstands in sea level, because the carbonate production is more prolific when the platform top is flooded (*i.e.*, 'highstand shedding', Droxler and Schlager, 1985; Schlager et al., 1994); (2) bottom currents form several contourite drifts along the Strait of Florida (Anselmetti et al., 2000; Mullins et al., 1980, 1987). These sedimentary bodies are associated with channels (called 'moats') and small-scale contourite-related sedimentary structures, such as sediment waves (Bergman, 2005); and (3) mechanical destabilisation of the slope is at the origin of numerous slides and bypass structures, such as gullies or canyons (Crevello and Schlager, 1980; Ginsburg et al., 1991; Mullins et al., 1984; Wilson and Roberts, 1995). These common sediment failures, expressed at different spatial and time scales along the deep sea Bahamian slopes, are associated with the overall prograding/aggrading trend of the Bahamian slopes since the Cenozoic (Eberli and Ginsburg, 1989; Harwood and Towers, 1988).

The objective of this study is to characterise the Mass Transport Complex (MTC) located on the northwest end of Little Bahama Bank (LBB), between 275 m and 460 m water depths, *c*. 10 km away from the top of the platform. At the present day, this MTC is partially buried and only a large head scarp 44 km long is visible on the sea bottom. However, its internal architecture, comprising several Mass Transport Deposits (MTDs), is revealed by the analysis of high resolution (HR) multichannel seismic lines. The latter provide details on the internal stratigraphy of an LBB extensional growth slope, which is built by both platform-derived downslope sedimentation and bottom current sedimentation since the Middle Miocene. The studied MTC is located in the upper part of a plastered drift and the infill of the associated depression seems to be influenced by bottom current circulation. In this paper, we provide a detailed characterisation of this MTC and discuss the potential linkages between off-bank transport, bottom current circulation and slope failures in the context of a leeward-carbonate slope.

2. Study area: general setting

The study area is located on the northern slope of LBB, at the northern extremity of the Bahamas (Fig. 1). LBB is the second largest isolated platform of the Bahamas (about 250 km long). It faces the Atlantic Ocean to the North, towards which it opens to the Blake Plateau. It is bordered to the east by the Blake Bahama Escarpment, to the west by the Strait of Florida and in the south by the NW and NE Providence Channel, which separates it from Great Bahama Bank (GBB) (Fig. 1).

2.1. Platform environment and platform margin

Along the windward open ocean margin of LBB, several Pleistocene eolianite islands (*i.e.* 'Cays') are associated with tidal delta oolitic shoals (Rankey and Reeder, 2011; Reeder and Rankey, 2008, 2009) (Fig. 2).

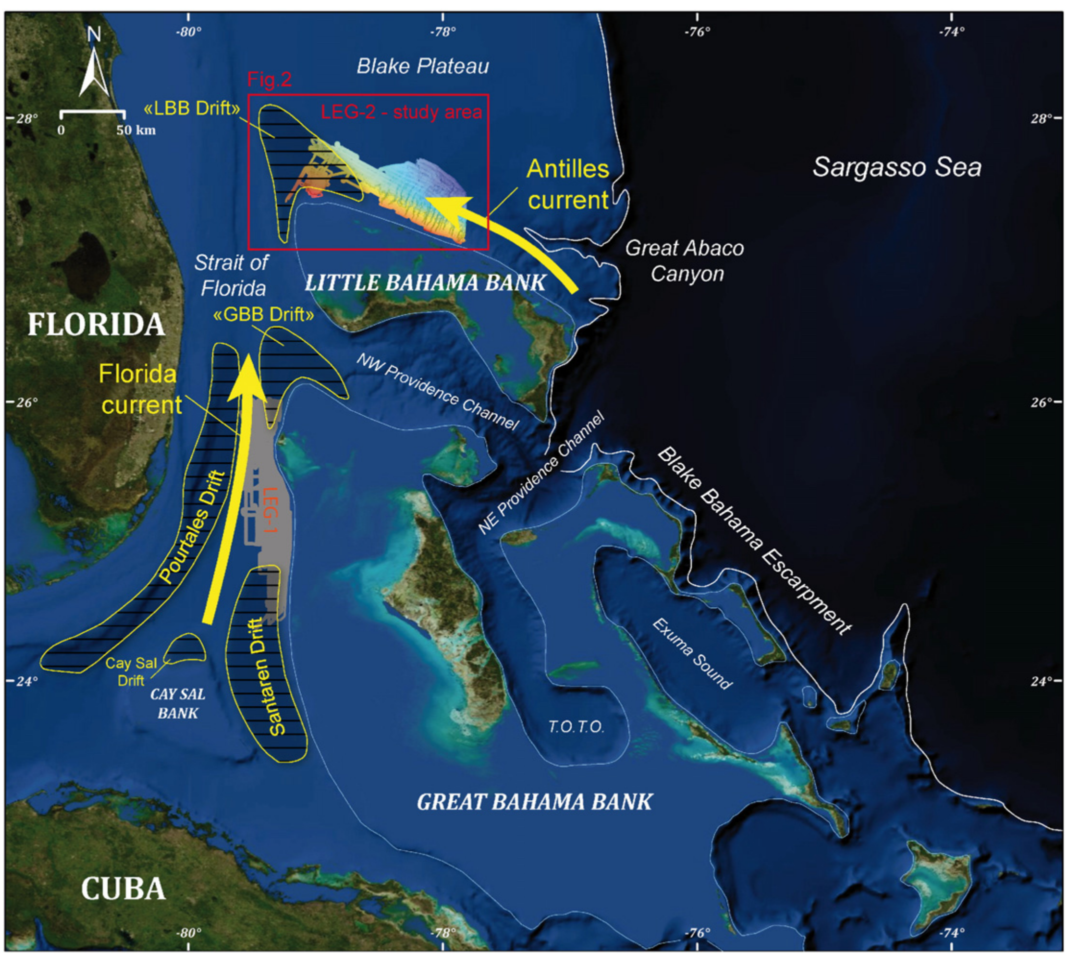

Fig. 1. Satellite image of the Bahamas, with locations of the Leg 2 (study area, Fig. 2) and Leg 1 of the Carambar cruise. The study area is influenced by two main oceanic currents, the Antilles Current, circulating along the northern slope of Little Bahamas Bank (LBB) and the Florida Current at the end of the Strait of Florida. Their combined action induces the onset of several contourite drifts.
Satellite image of the Bahamas is from © 2011 Microsoft Corporation and its data suppliers. The currents are redrawn from Mullins et al., (1980) and Bergman (2005).

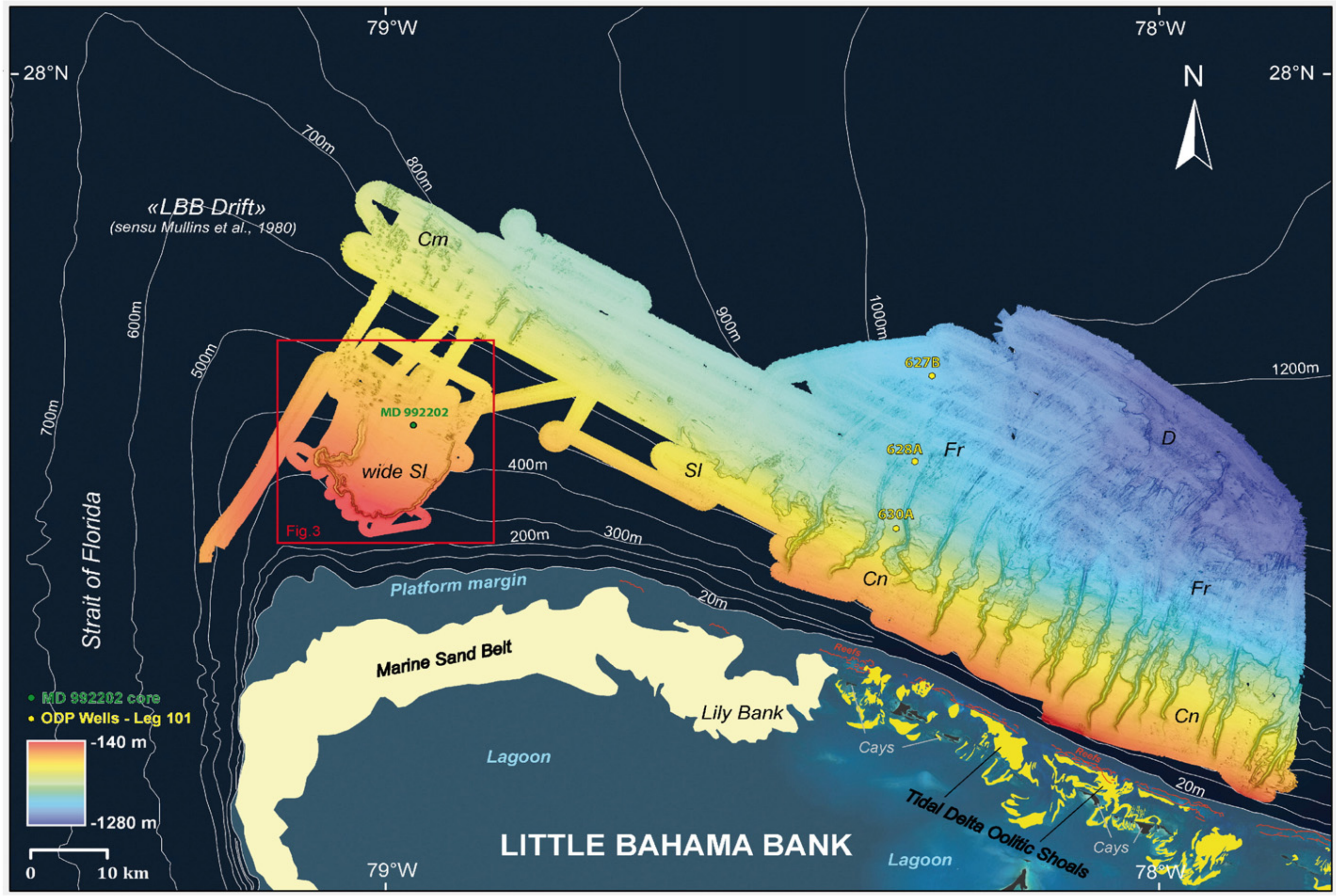

Fig. 2. Bathymetrical map of the Leg 2 (Carambar cruise) covering the northwest slope of Little Bahamas Bank (LBB) showing the location of the study area, *c.* 10 km away from the platform. It reveals contrasted morphologies with an eastern part showing a dominance of bypass architectures, whereas the western part mostly comprises depositional features. Upstream of the study area, the platform is also marked by contrasted features, with discontinuous marginal reefs associated with tidal delta oolitic shoals on the eastern part, becoming absent on the western part, where a marine sand belt develops. The main morphological elements seen on the study area are the following: *Cn*: canyons, *Fr*: distributary furrows; *D*: depositional area; *Sl*: slide; *Cm*: cold-water coral mounds.

Previous studies (Hine, 1977; Reeder and Rankey, 2008) showed that a complex interaction exists between the eolianite islands, the oolitic sand shoals and discontinuous Holocene barrier reefs, located a few kilometres northward from the islands (Fig. 2). These reefs and islands induce a restricted and focused tidal flow energy, which is controlling shoal development. On the western part of the bank margin, reefs are sparser and become absent towards the northwestern end of LBB. In this area, a marine sand belt developed during the Holocene, the eastern part of which is called Lily Bank (Fig. 2), consists of an active oolitic tidal sand shoal (Ball, 1967; Hine, 1977; Rankey and Reeder, 2011; Sparks and Rankey, 2013). The platform margin including the uppermost slope environments reaches down to 240 m water depth (Rankey and Doolittle, 2012) and its development is by a complex interplay of bypass, erosional and depositional processes. Rankey and Doolittle, 2012 describe the occurrence of terraces delimited by escarpments which are affected by several collapses that are onlapped by a thick Holocene sediment wedge.

2.2. The morphological features of the northern slope of Little Bahama Bank

The steep uppermost slope of LBB opens to the northern slope basin system, which was the focus of several studies in the 80s (*e.g.*, Harwood and Towers, 1988; Mullins et al., 1984; Schlager and Ginsburg, 1981; Van Buren and Mullins, 1983). Based on the present-day slope profile, the northern slope of LBB has been defined as an accretionary carbonate slope (Schlager and Ginsburg, 1981) and has been prograding northward since the early Miocene (Harwood and Towers, 1988). However, it showed evidence for some significant bypass since the Pliocene (Harwood and Towers, 1988; Van Buren and Mullins, 1983) and these sedimentation patterns have been classified as a base-of-slope apron system (Mullins and Cook, 1986; Mullins et al., 1984).

In terms of main morphological features, our new high-quality survey revealed a series of sediment transport architectures along the LBB slope. It consists of short gravity systems (about 40 km long) in its eastern part, which has a far more complex sedimentary structure than originally suggested by early studies. These interpreted the structures as gullies or small linear canyons (Harwood and Towers, 1988; Mullins et al., 1984; Van Buren and Mullins, 1983). Our study shows that they consist of true submarine canyons that can incise over up to 150 m depth. These canyons open to several shallow distributary furrows that feed several depositional areas situated downslope (Fig. 2). The western part of the study area comprises a completely different morphology compared to the eastern part and shows a semi-conical body of carbonate sands, situated at the northwest corner of LBB and previously interpreted as a contourite drift ('LBB Drift', Mullins et al., 1980) (Fig. 2).

2.3. Oceanic circulation and contourite drifts

The western part of the LBB northern slope (previously called 'LBB Drift') has been prograding northward as the result of both Florida and Antilles currents (Mullins et al., 1980), and is therefore a good example of the key role that oceanic circulation has in shaping Bahamian deep-water sedimentation. The evolution of oceanic currents through time and space, since the initiation of the Loop current during the progressive closure of the Isthmus of Panama during the middle Miocene (Mullins et al., 1987), can alternatively induce sediment erosion, bypass or deposition of contourite drifts from the Gulf of Mexico to the Strait of Florida. Evidences of the initiation of the Loop current are visible on the west Florida carbonate ramp, and this event is recorded by a major erosional surface dated at approximately 12–15 Ma (Mullins et al., 1987). Since then, the carbonate sedimentation abruptly changed from a unit of prograding clinoforms to a pelagic 'slope-front-fill' system (Mullins et al., 1987). In the Strait of Florida, Bergman (2005) identified the initiation of four contourite drifts since 12.2 Ma: the Pourtales Drift, the Santaren Drift, the Cay Sal Drift and the GBB Drift (Fig. 1). The Pourtales and Santaren drift growth, between 12.2 Ma and 3.6 Ma, is driven by the thermohaline circulation (Bergman, 2005). Subsequently, at about 3.6 Ma, the Santaren Drift shifted towards the GBB slope in response to a lateral migration of bottom-currents (Bergman, 2005), probably induced by the definitive closure of the Isthmus of Panama at 3.5 Ma (Coates et al., 1992; Haug and Tiedemann, 1998; Steph et al., 2006) and by enhanced sea-level fluctuations associated with the Late Pliocene main intensification in Northern Hemisphere Glaciation (Bergman, 2005; Reijmer et al., 2002).

3. Dataset and methods

This study has been conducted on a dataset collected during the Carambar cruise—Leg 2 (Nov. 2010) with the *R/V Le Suroît* (Mulder et al., 2012a,b). Bathymetric data of the LBB slope were acquired using a Kongsberg EM302 multibeam echosounder, processed using *CARAIBES* software (©Ifremer), and analysed using ArcGIS software (©Esri). The spatial resolution of the resulting bathymetrical map is 20 m × 20 m and has a vertical resolution of 1 m.

In total, 600 km of very high-resolution (VHR) seismic profiles (vertical resolution lesser than 0.5 m) were acquired across the large slide using a sub-bottom profiler (Chirp mode). Two profiles (lines 225 and 233, Figs. 3 and 5) were calibrated for the sediments covering the last 375 kyr, using the MD992202 core (26 m long) collected during the Interpole cruise on the *R/V Marion Dufresne* (Lantzsch et al., 2007; Figs. 2 and 3).

High resolution (HR) 2D seismic data, 115 km in total, with a vertical resolution of about 3 m, were interpreted using the classical seismic stratigraphy analysis. The vertical depth scale can be approximated using an average velocity of 1700 $m \cdot s^{-1}$ for the periplatform sediments (Harwood and Towers, 1988; Mullins et al., 1980; Sheridan et al., 1966). Hence, 60 ms *twt* corresponds to approximately 100 m. Three ODP wells (630A, 628A and 627B, leg-101, Austin et al., 1986; Fig. 2) were used to calibrate the HR 2D seismic data from the early Eocene–late Paleocene hiatus up to the sea bottom.

This dataset allows a detailed characterisation of variations in sediment patterns at different time and space scales. Bathymetrical analysis and interpretation of the VHR seismic lines help to understand the modern morphologies and the associated sedimentary processes in the western part of the LBB slope. Analysis of the HR 2D seismic lines allows investigating the ancient subsurface architectures.

4. Results

4.1. Surface morphology

4.1.1. General morphological characteristics of the seafloor

The large circular escarpment occurs in the northwestern part of the study area, 10 km away from the top of the platform (Fig. 2). This feature is located on the upper slope between 275 m and 460 m water depths and is 12 km wide (Fig. 3). It shows an overall semicircular shape, and a total length of 44 km. Its eastern part has a linear shape with a sinuosity of 1.26, whereas its western part presents a meandering shape with a sinuosity of 1.82 (Fig. 3). Five profiles reveal that the structure has an almost vertical external edge (from 40 to 70 m high), which is higher and steeper than the internal edge, as displayed by asymmetrical U-shaped transverse profiles (Fig. 3; profiles 1 to 5).

Inside the wide scar, the slope ranges from 1° to 0.6° after an intra-slope break situated at 360 m water depth (Fig. 3; profile 6). Within the structure, towards the meandering part, two smaller scale slide scars, 1 to 2 km wide, occur suggesting several secondary collapses of the internal edge (Figs. 3 and 4). The corresponding VHR seismic line 242 displays small-scale slide scars and their resulting deposits that occur both inside the scar and at the toe of the internal edge (Fig. 4). Similarly, the transverse bathymetrical profile 3 shows an isolated topographic high on the internal edge that probably results from small sediment failures (Fig. 3). The composite line 243–244 displays several slide scars and their associated displaced sediments against an isolated topographic high (Fig. 4).

All these seafloor features show that a contrast exists between the sediments inside the wide circular scar and those of the steep external edge. Despite the significant vertical character of the latter, evidence of recent collapse events is only present on the gentle internal edge.

4.1.2. VHR seismic features and lithology

VHR seismic lines 225 and 233 display two seismic units that are characterised by very distinct echo facies (Fig. 5). (1) Unit 1, visible at the base of the profiles, is bounded at its top by a major unconformity and is onlapped by Unit 2. Unit 1 is transparent with some discontinuous reflections and overlapping hyperboles (lines 225 and 233, Fig. 5). Unit 1 cuts to the seafloor and forms the steep edge of the scar (on line 233, Fig. 5), as seen on the bathymetrical map (localisation on line 233, Fig. 3). (2) Unit 2 is characterised by continuous layered reflections (echo-facies I.B. of Damuth, 1980; Mullins et al., 1979) and can be subdivided into sub-units 2a and 2b, which are separated by an erosional surface (Fig. 5). VHR seismic lines 225 and 233 are calibrated with a core that was taken 25 m away from line 225 (Fig. 5; Lantzsch et al., 2007). The sediments consist of periplatform ooze and coarser intervals with cemented debris. Latter intervals contain massive, poorly sorted, mud-supported or clast-supported deposits with increased high-Mg–calcite content (Lantzsch et al., 2007). The intervals of cemented debris seem to correspond to very high amplitude reflections on the VHR seismic data (Fig. 5). Lantzsch et al. (2007) identified 11 marine isotope stages (375,000 years) in the core that penetrates Unit 2a and part of Unit 2b.

4.1.3. Fluid circulation evidences

Unit 2a exhibits irregular undulating reflections, interpreted as reflecting deformed deposits which are visible not only in the subsurface (lines 225 and 233, Fig. 5) but also on the surface, at the end of the eastern branch of the circular escarpment (line 253b, Fig. 6). The top of Unit 1 shows a complex shape and notably forms a paleotopography that seems to be in continuity with the isolated topography observed on the seafloor (profile 5, Figs. 3 and 6). Deformed deposits are often associated with circular depressions on the seafloor, in front of the wide incision between 450 m and 570 m water depths (Fig. 3). These structures are interpreted as pockmarks (Figs. 7 and 8) and have an average diameter of 180 m (average surface of 42,000 m^2) and an average depth of 11 m and occur associated with topographic highs interpreted as cold-water coral mounds (Fig. 7). On the VHR seismic line 239, pockmarks are characterised by a V-shaped depression beginning on top of Unit 1 and cutting through Unit 2 (Fig. 7).

The map of the vertical edge shows that it continues deeply downslope of the eastern branch. However, it is partially covered by recent sediments (Fig. 8). The map further shows the spatial distribution and relationships between the deformed deposits and the pockmarks situated in front of the wide slide.

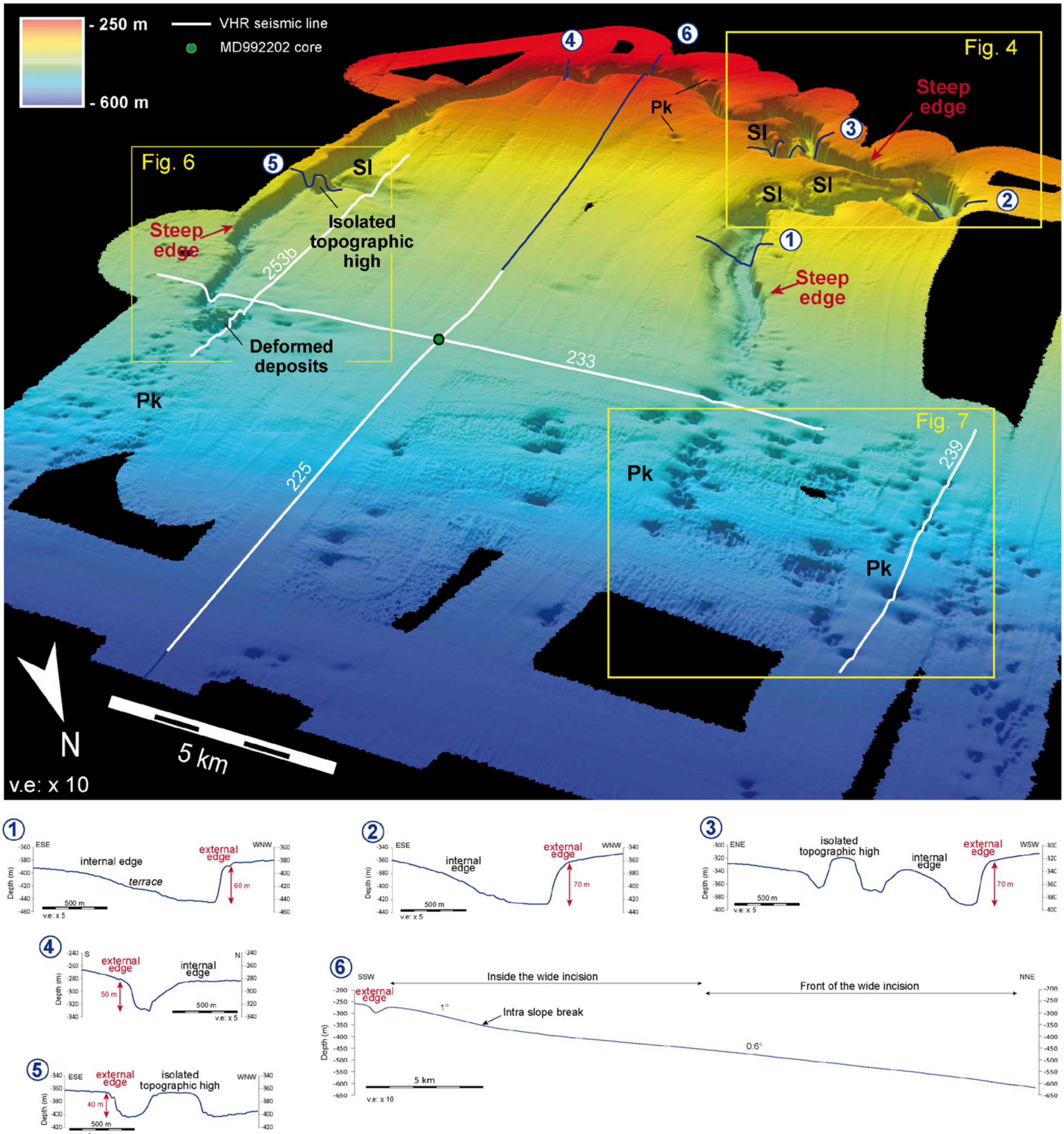

Fig. 3. 3D bathymetrical map focusing on the wide incision and showing the location of bathymetrical sections (noted from 1 to 6) and VHR seismic lines. The wide escarpment, located between 275 m and 460 m water depths, presents a semicircular shape composed of an isolated meandering shape on the western part. The bathymetrical profiles typically have an asymmetrical U-shape, with an almost vertical external edge, from 40 to 70 m high. Several small-scale slides (Sl) are visible inside the wide scar and several pockmarks (Pk) are present in front of the scar. Detailed views of these elements are proposed in Figs. 4, 6 and 7, the locations of which are indicated on this 3D view.

4.2. Subsurface analysis

4.2.1. Stratigraphic seismic units

Using a classical seismic stratigraphy approach, seven units have been identified on the HR seismic lines (Fig. 9) within the interval comprised between the early Eocene–late Paleocene hiatus (top Unit E of Austin et al., 1986; Fig. 10) and the present day sea bottom. Unit A is equivalent of Unit D of Austin et al. (1986) the top of which is a regional erosion surface interpreted as a late Oligocene–middle Miocene hiatus (Austin et al., 1986; Sheridan et al., 1983). Units B to G could not be correlated with the seismic units of Austin et al. (1986) and hence could not be calibrated with the ODP wells positioned along the northern slope of LBB. Therefore, ages of the boundaries of units B to G illustrated on the Fig. 10 may have some uncertainties.

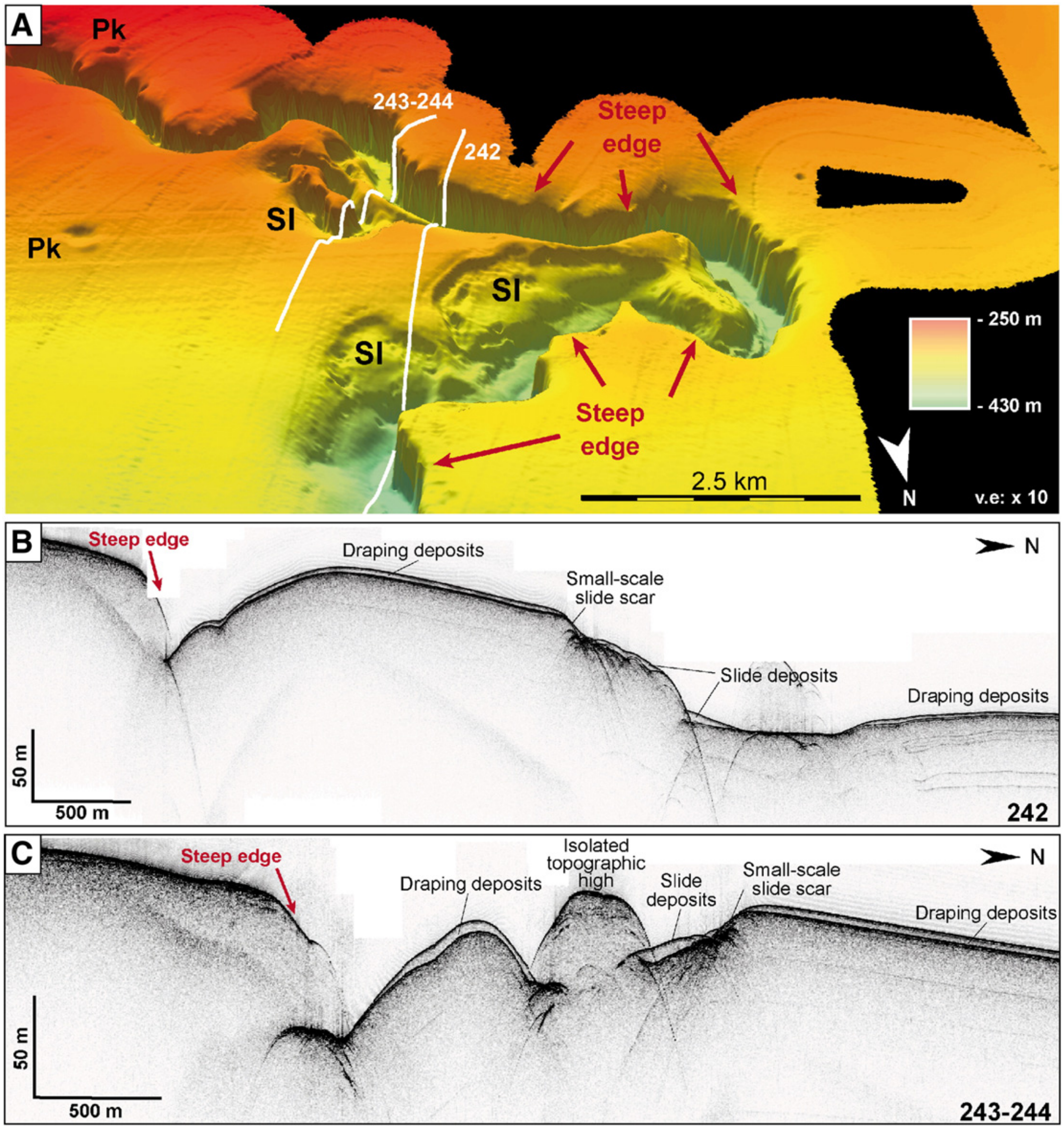

Fig. 4. Close-up on the 3D bathymetrical map showing the small-scale slides affecting the internal edge of the breakout area (A) and on VHR seismic line 242 (B) and composite lines 243–244 (C). These slides are 1 to 2 km wide and are associated with slide deposits inside the scar and at the toe of the internal edge.

Seismic units B to D form an aggrading and prograding depositional sequence towards the north (line 77, Fig. 11). Boundaries of these units are defined by onlap and downlap terminations of seismic reflections and delimit several sigmoidal clinoforms. The top of Unit D is characterised by an erosional surface after an offlap break and is filled by a slide mass showing continuous, low amplitude wavy reflections. Seismic facies of Units B to D are mainly characterised by an alternation of very continuous and discontinuous reflections with a low to high amplitude, and could be interpreted as periplatform ooze accumulations and gravity flow deposits, respectively. Unit E thickens towards the SE. It contains continuous to discontinuous reflections downlapping onto Unit D (Figs. 11 and 12). The key feature to understand the large circular geometry of the seafloor lies within Unit F. It consists of three seismic facies related to three distinct depositional environments and/or architectural elements: the plastered drift, Mass Transport Deposits (MTDs) and upper slope deposits (Figs. 11 to 13). Finally, Unit G overlaps Unit F and fills the circular depression (Figs. 11 and 12). These two last seismic units show complex geometries that result from a series of sedimentary processes, described in the following section.

4.2.2. Unit F — plastered drift

Unit F is aggrading and characterised in its lower part, 550 to 800 m below the present-day sea level, by continuous parallel reflections, which onlap Unit E and downlap onto the bottom set of Unit D (Figs. 11A, B, 12B and C). The configuration of reflection terminations indicates both down and upslope migrations, which are characteristic of plastered drifts (Faugères et al., 1999). The top of Unit F is characterised by a major erosional surface (Figs. 11, 12C and 14). This surface is associated with common cold-water coral mounds in the distal part of the slope (Fig. 14) that seem to use this irregular surface as a substratum (Correa et al., 2012). After the offlap break of Unit F, the erosional surface is associated downslope with slide sediments affected by normal faults and small thrusts in front of sigmoidal clinoforms (Figs. 11A and 14).

4.2.3. Unit F — Mass Transport Deposits (MTDs)

In the middle part of Unit F (around 500 m below the present-day sea level), the seismic facies with continuous parallel reflections abruptly passes over into a chaotic seismic facies. This facies change is marked by a vertical limit of 60 ms (*twt*) high, underlining a truncation of

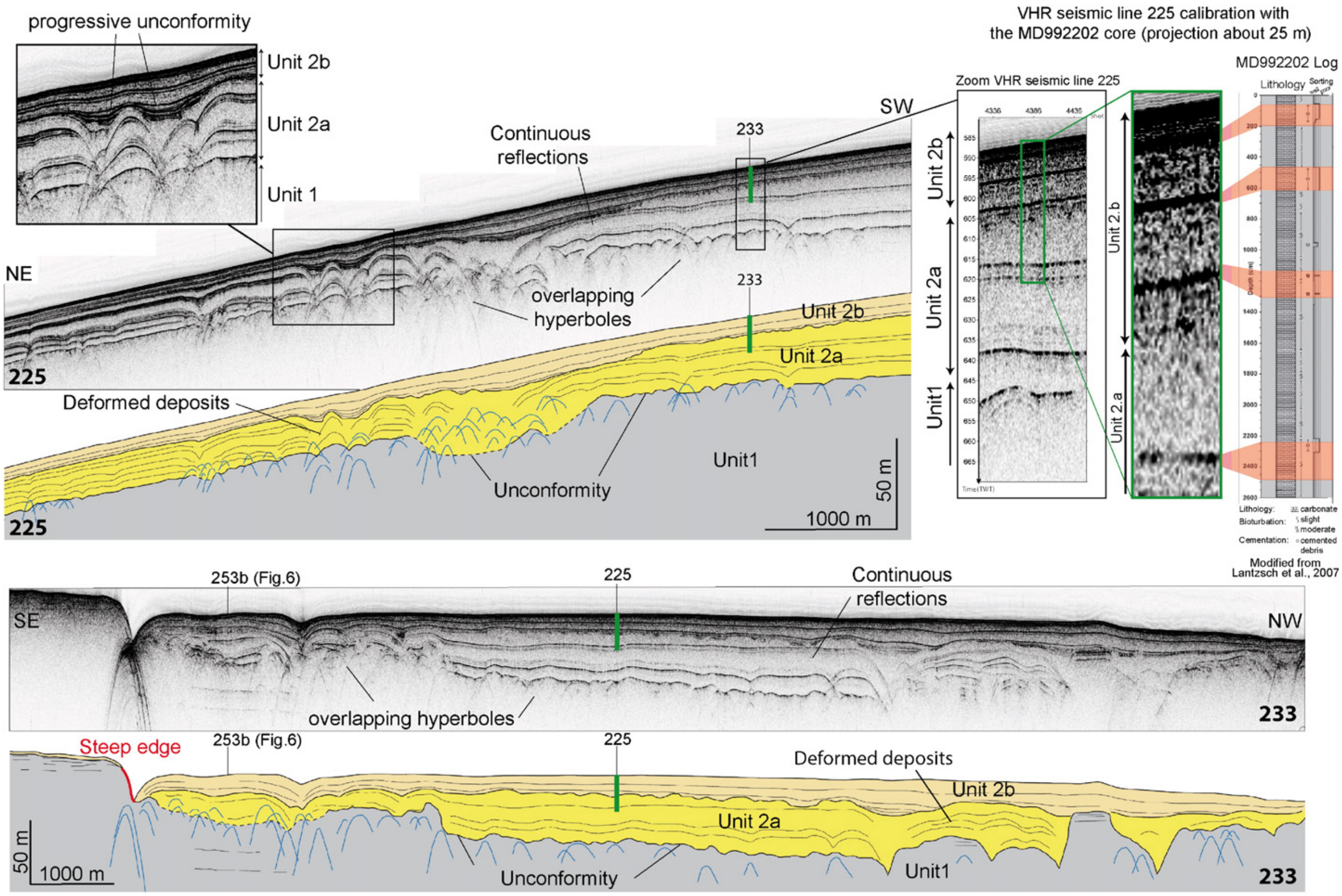

Fig. 5. VHR seismic lines 225 and 233 (see in Fig. 3 for location) calibrated with the MD992202 core (Lantzsch et al., 2007), showing two major units (see text for details). The top of Unit 1 is an unconformity surface associated with several overlapping hyperboles. Unit 2 is characterised by continuous bedded reflections, corresponding to the alternation between periplatform ooze and cemented debris intervals. Four cemented intervals (see MD992202 log) have been identified as the very high amplitude reflections seen on the VHR seismic line.

reflection terminations (line 77, Fig. 11B and line 80, Fig. 12B). The thickness of this chaotic seismic facies decreases upslope forming a wedge onlapping Unit E (line 77, Fig. 11 and line 79, Fig. 12A). The thickness and deformation of the chaotic mass is more important against the vertical limit (between 450 and 500 m below the present-day sea level), which is likely to indicate that the chaotic mass is compressed against this surface.

Based on the disorganised and discontinuous character of the seismic facies compressed on the vertical limit, the chaotic mass is interpreted as Mass Transport Deposits (MTDs) (Weimer, 1989). Given their overall geometry, these MTDs are considered as frontally confined (*sensu* Frey-Martínez et al., 2006) inside Unit F. The vertical limit between the two facies can reach a height of up to 140 ms (*twt*), and represents the frontal and lateral edges of the slide (line 77, Fig. 11B and line 81, Fig. 12B), whereas the thickest part of the MTDs corresponds to the compressional frontal part.

4.2.4. Unit F — upper slope deposits

Outside the wide incision the upper part of Unit F (between 250 m and 400 m below the present-day sea level) shows a seismic facies characterised by discontinuous reflections of low amplitude, with downlap terminations and small-mounded reflections (Figs. 11C, 12A and 13). This seismic facies is interpreted to represent upper slope deposits, composed of sediment transferred from the platform, whilst the small mounded reflections are interpreted as blocks/boulders detached from the platform margin or the uppermost slope (Rankey and Doolittle, 2012). Another evidence for the detached block interpretation is the concave shape of the platform margin, upslope of the large slide (Figs. 2 and 9), the so-called 'scalloped margin' of Mullins and Hine (1989) that generates isolated blocks or mega-breccias because of this type of platform erosion.

A progressive interfingering between the upper slope facies and the plastered drift facies is shown in line 80 (Fig. 13). This illustrates the complex contact between the drift deposits and the upper slope deposits.

4.2.5. Unit G — filling unit

HR seismic Unit G corresponds to VHR seismic Unit 2 (Fig. 10). Unit G is aggrading, thickens upslope and is characterised by high amplitude, very continuous reflections, downlapping onto Units F and E (Figs. 11 to 14). The comparison with the stratigraphy of Lantzsch et al. (2007; Fig. 5) suggests that it consist of fine-grained sediment; most likely periplatform ooze deposits.

The upper part of the wide depression (between 300 m and 360 m below present-day sea level), near the circular scarp, shows two types of channelised geometries (lines 77 and 79, Figs. 11C and 12A). (1) The first type is located against the escarpment and the channel appears to be associated with lateral overspill deposits (line 77, Fig. 11C). The wedge-shaped geometry of this feature shows large similarities with a levee complex. These geometries also induce an intra-slope break on the seafloor at 360 m water depth, marked by a change in slope gradient from 1° to 0.6° (profile 6, Fig. 3). (2) The second type of channel, located near the meandering part of the slide scar, displays aggrading geometries (line 79, Fig. 12A). These channelised geometries are likely to be small-scale slides imaged in a strike section or, alternatively, buried pockmarks (line 79, Fig. 12A). Under the meandering

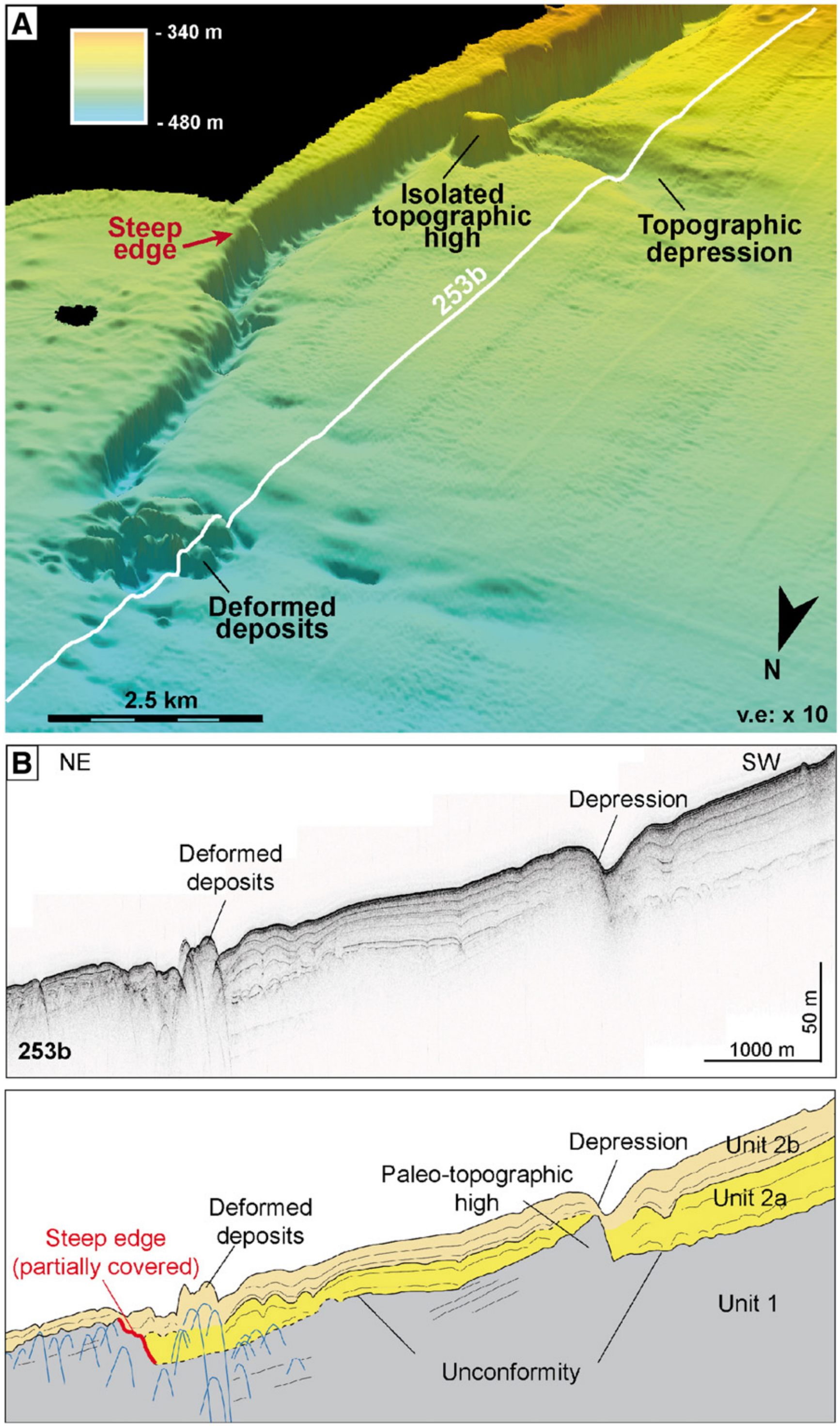

Fig. 6. Detailed view of the deformed deposits situated against the partially covered steep edge of the incision, observed on the 3D bathymetrical map (A) and on VHR seismic line 253b (B). The unconformity surface, characterising the top of Unit 1, shows a paleo-topographic high that seems to be the continuation of the isolated topographic high observed on the seafloor.

part, erosion surfaces affected Unit C and D. These erosion surfaces have an extension of about 4 km and mark the unstable character of sediment deposited prior to the MTC formation (line 79, Fig. 12A).

Finally, Unit G is affected by several normal faults observed along the entire slope with a small offset (less than 10 ms *twt*) and associated with wavy reflections (line 77, Fig. 11 and line 79, Fig. 12A).

The HR seismic analysis allowed identifying and reconstituting the complex architectures of the different stratigraphic units (Fig. 14). The next section proposes to reconstitute the wide slide origin and its evolution.

5. Discussion

5.1. Re-evaluation of the ‘LBB Drift’ (sensu Mullins et al., 1980)

The ‘LBB Drift’ has been defined by Mullins et al. (1980) on their line 3′, located in the westernmost part of the study area (Fig. 9). These authors dated the unconformable base of the ‘LBB Drift’ to the middle Miocene based on correlation with the JOIDES drill holes on the Blake Plateau (Schlee et al., 1979). The large contourite body described by Mullins et al. (1980) spatially and temporally corresponds to the

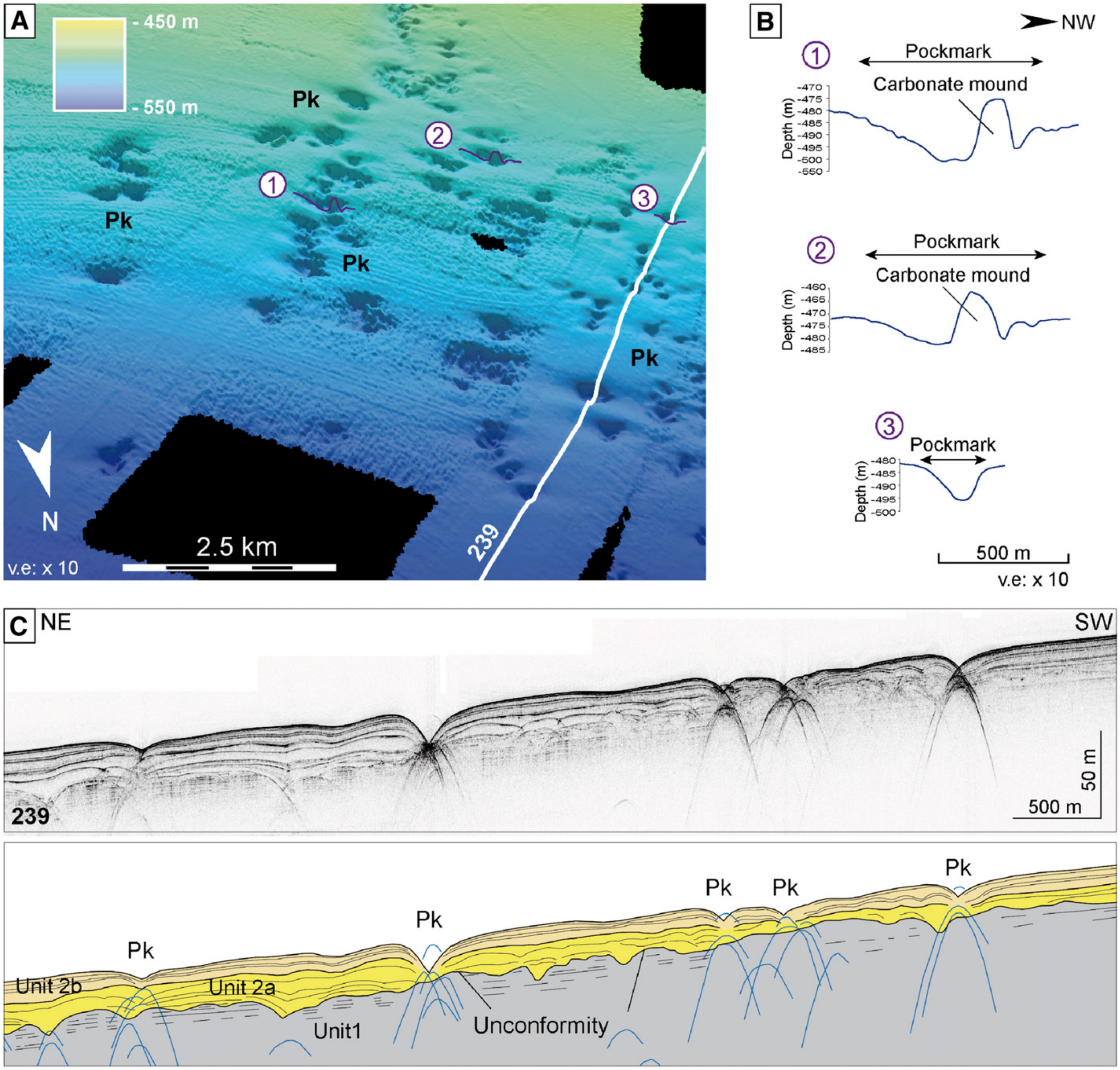

Fig. 7. Detailed view of the pockmarks (Pk) located in front of the wide incision, between 450 m and 570 m water depths, from the 3D bathymetrical map (A), transverse profiles (B, numbered from 1 to 3) and VHR seismic line 239 (C). These pockmarks have an average depth of 11 m and can be associated with isolated topographic highs, interpreted as cold-water coral mounds (A and B). Pockmarks present a V-shape and are located above overlapping hyperboles (C).

northern slope of LBB illustrated on line 77, which shows seismic Units B to G. Mullins and Neumann (1979) defined the sedimentation patterns in the western part of the northern slope of LBB as an '*extensional growth slope*' which comprises sedimentary units built by the lateral transport driven by bottom currents (Florida Current and Antilles Current) as well as off-bank transport from the platform. Units B to D seem to be dominated by platform-derived downslope sedimentation, showing an alternation of periplatform ooze and gravity flow deposits, whereas Unit F displays very continuous reflections with both upslope and downslope migrations. Therefore, based on these characteristics, Unit F is the only unit within this extensional growth slope (*i.e.* 'LBB Drift' of Mullins et al., 1980) that is arguably built by contour currents, and would agree with a plastered drift (*sensu* Faugères et al., 1999). This new definition, thanks to the new HR-multichannel seismic, allows clarifying the sedimentary dynamics of the LBB extensional growth slope ('LBB Drift' *sensu* Mullins et al., 1980), which is not only controlled by bottom currents. Consequently, we refer to Unit F as a 'plastered drift' unit throughout the discussion.

5.2. Slide initiation and evolution

A four step-model of the slide formation and evolution is proposed (Fig. 15). (1) The first step corresponds to contour current sedimentation alternating, in the upslope part, with input of sediments derived from the platform. (2) The second step is the formation of the scarp and associated MTDs. Their origin appears complex and can result from several combined processes. (3) The third step is the infill of the depression. At this stage, the deposits are still affected by the motion

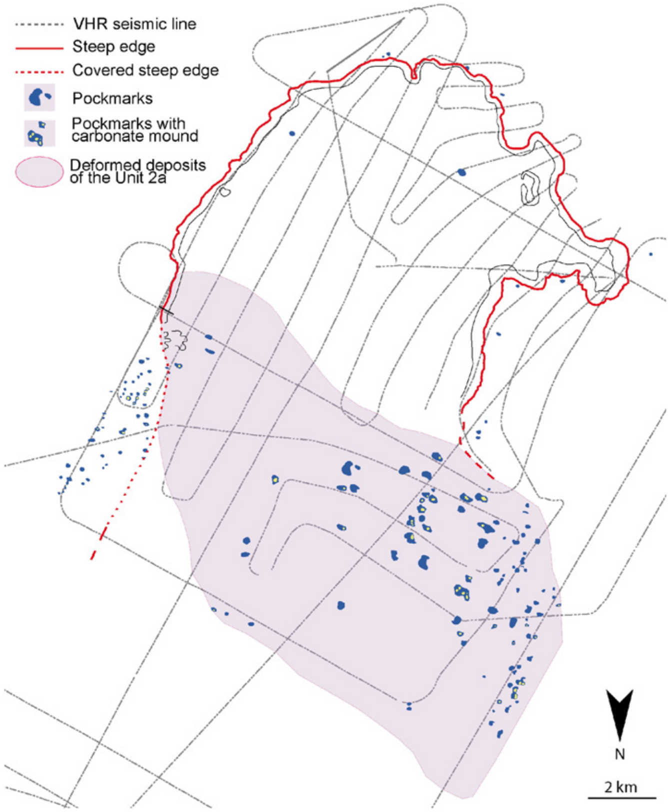

Fig. 8. Map of the semicircular steep edge and spatial distribution of the deformed deposits of Unit 2a as well as the pockmarks in the front of the wide scarp.

of the underlying MTDs. Fluid escapes, originating from the underlying MTDs' compressive area, deform the infilling sediments and form pockmarks. (4) Finally, the fourth step corresponds to the morphology seen on the present-day seafloor, which shows an evolution of sediment infill and the formation of small-scale slope failures.

5.2.1. Step 1: initial plastered drift geometry and transitional contact with upper slope sediments

Before its destabilisation, Unit F onlapped the top of Unit E. The top of Unit E corresponds to the unconformity situated roughly within the Pliocene interval (Figs. 10 to 14).

Unit F shows both upslope and downslope migrations and corresponds to a plastered drift (*sensu* Faugères et al., 1999). The HR seismic interpretation shows the lateral and frontal drift terminations at about 800 m below the present-day sea level (Fig. 14). The contact between the plastered drift and the upper slope deposits seems to be complex as shown in line 80 (Fig. 13). The transitional contact may be induced by the interaction between contour current sedimentation and sediment supply from the platform (step 1, Fig. 15). These variations can be the result of the fluctuating intensity of contour currents, of variable carbonate sediment productivity on the platform or variations in sediment transport from the platform.

5.2.2. Step 2: origin of the escarpment and the MTDs

The escarpment formed as a result of large-scale slope instability (step 2, Fig. 15) and locally shows the meandering character of the head scarp and the spatial distribution of the associated MTDs. These MTDs are frontally confined inside the plastered drift and are delimited by both frontal and lateral edges (Figs. 11 to 15). To explain the MTC geometries two hypotheses are proposed.

(1) The first hypothesis implies the extensive slide that affected the upper part of Unit F (step 2 — hypothesis 1, Fig. 15). In this scenario, the semicircular escarpment is the head scarp of the MTC and the chaotic facies would represent slide deposits. The sinuous shape of the head scarp would suggest that the slide represents a succession of several mass-failure events, and the main head scarp would be the result of coalescing small failure scars. The curious meander present in the western part of the wide

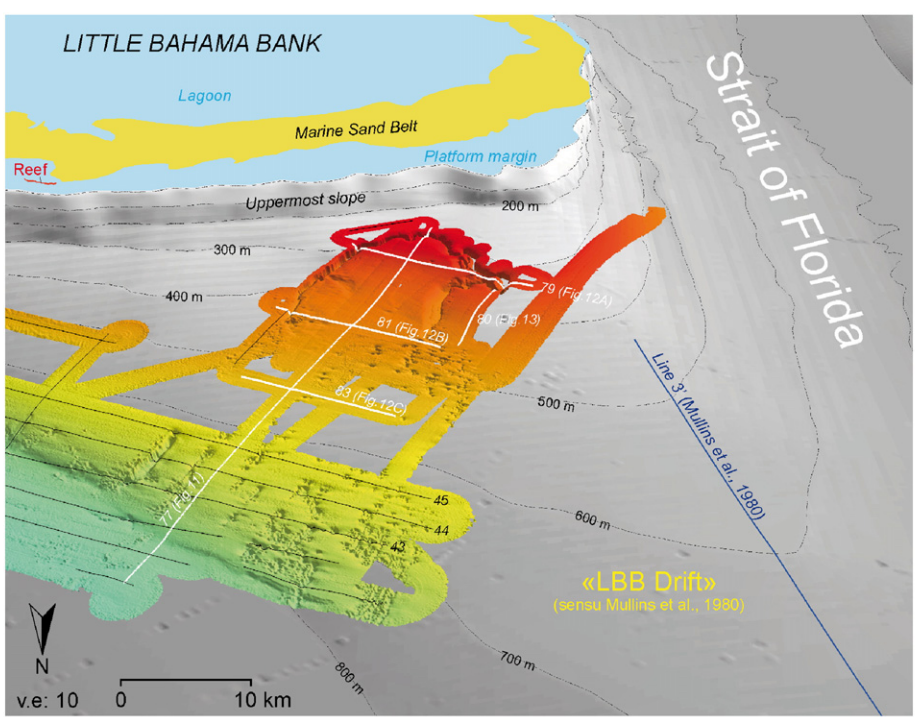

Fig. 9. Location of the HR seismic lines on the 3D bathymetrical map of the study area superposed on a regional bathymetrical reconstitution. The LBB Drift has been previously identified by Mullins et al. (1980) on their line 3′, located along the drift growth axis.

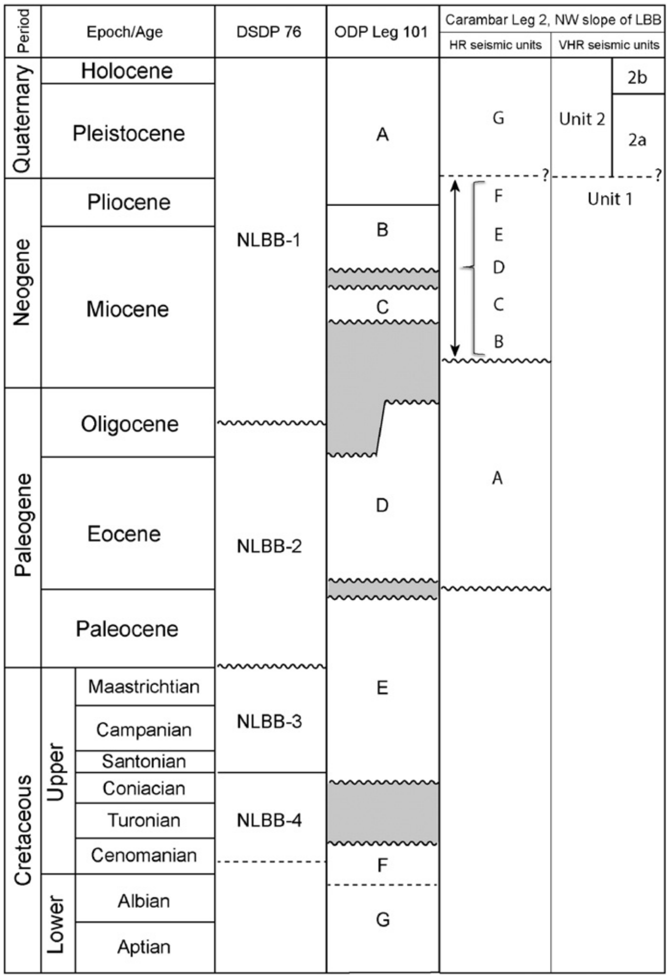

Fig. 10. Relationships between the seismic units of the northwest corner of LBB slope (defined in this study), the NLBB depositional sequences of DSDP leg 76 (Van Buren and Mullins in Sheridan et al., 1983) and the seismic sequences of ODP leg 101 (Austin et al., 1986). Wavy lines represent unconformities, grey intervals represent stratigraphic hiatus and dashed lines represent uncertain boundaries.

incision likely resulted from a local instability merging with the large slide. In the meandering part, the local erosional surfaces affected Units C and D before the onset of the MTC. These observations attest to an unstable character of this part of the MTC. Contradicting the first hypothesis as main mechanism forming the slide are the small amount of slide sediments compared to the height of the head scarp and the space created (Figs. 11 and 14).

(2) The second hypothesis considers the MTC as originating from the combined action of bottom currents and gravity processes. In this case, the escarpment could result from bottom current activity along the slope, simultaneously with or succeeding the wide slide formation (step 2 — hypothesis 2, Fig. 15). Such currents would induce major erosion along the head scarp and would cause a potential reworking of MTDs (step 2 — hypothesis 2, Fig. 15). In addition, the top of Unit F is consistently affected by a major erosional surface in the distal part of the plastered drift (Fig. 14). This observation is thought to be additional evidence to support the hypothesis of a period with significant erosion by bottom currents during the Pliocene (approximately).

In the Strait of Florida, an intensification of the Florida current was evidenced by a shift of the Santaren Drift (Fig. 1) towards the GBB slope (Bergman, 2005). Bergman (2005) identified the onset of the contourite drift shift at about 3.6 Ma and Reijmer et al. (2002) distinguished two erosional horizons dated at 4.6 and 3.3–3.6 Ma. These observations have been interpreted to result from the definitive closure of the Isthmus of Panama at 3.5 Ma (Coates et al., 1992; Eberli et al., 1997; Reijmer et al., 2002) in combination with enhanced sea-level fluctuations associated with the Late Pliocene main intensification in Northern Hemisphere Glaciation (Haug and Tiedemann, 1998). However, the study area is not located directly in the Florida Current pathway but within those of the Antilles Current. Therefore, the observations made along the Strait of Florida by previous studies (Anselmetti et al., 2000; Bergman, 2005; Betzler et al., 1999; Reijmer et al., 2002) can not directly be extrapolated to the northern slope of LBB.

The origin of the semicircular escarpment and the MTDs is therefore highly contentious. It can be the result of gravity sliding and/or bottom current erosion. These two processes may have occurred simultaneously or may have alternated. However it remains difficult to confidently identify the role played by each process in shaping the encountered morphological features.

5.2.3. Step 3: filling depressions

The downlap configuration of Unit G on Units F and E indicates that deposition of Unit G occurred after MTC formation whilst the Unit G sediments fill up the large depression (Figs. 11C, 12 and 14). The channelised geometries present close to the escarpment are associated with lateral overspill deposits and suggest that bottom currents eroded the escarpment and deposited sediment along the slope (Figs. 11C, 12A and step 3, Fig. 15). These currents can have different origins (blue arrows in the step 3, Fig. 15). They either may relate to the activity of the Antilles Current or could be seasonal and local hyperpycnal waters plunging downslope, the density cascading process described by Wilson and Roberts (1992, 1995) or waters associated with the Gulf Stream Ring (Richardson, 1983; Richardson et al., 1978).

In addition, deformed deposits and pockmarks are present within Unit G (step 3, Fig. 15). Their spatial distribution reveals a clear relationship between deformed deposits and the pockmarks situated in front of the head scarp above the compressional area of the MTC (Fig. 8). The fluid circulation at the origin of pockmarks can be induced by compression of sediment against the frontal edge of the MTC resulting in the expulsion of their interstitial waters, forming pockmarks during its upward motion. Hence, the deformed deposits associated with the pockmarks could be formed by this fluid expulsion process. Alternatively, it can be induced by creeping processes linked to the motion of the MTDs (Figs. 5 to 8 and 14).

5.2.4. Step 4: small-scale failures of the filling unit

The last step (step 4, Fig. 15) represents the present-day modern sedimentation processes as shown by the seafloor morphology (Fig. 3). This final step corresponds to Unit 2b, identified on the VHR seismic lines (Figs. 5 to 7) and is dated to Holocene and Late Pleistocene (Lantzsch et al., 2007, Fig. 5). The sediments infilling the depressions seem to have a very unstable nature. The upper part of the sediment infill is affected by several small failures (1 km to 2 km wide) which give the wide slide a complex geometry (Figs. 3 and 4). Moreover, this unstable character is also expressed by several normal faults, affecting Unit G along the whole slope (line 77, Fig. 11A and C, line 79, Fig. 12A).

5.3. The sedimentary dynamic of the LBB northwest corner slope

The discontinuous Holocene barrier reefs on the windward northwest open margin of LBB induce a restricted and focused tidal energy that allows the upstream development of oolitic tidal shoals (Rankey and Reeder, 2011; Reeder and Rankey, 2008, 2009). It also focusses the transfer of sediment from the platform onto the slope. In the northwest corner of the LBB margin, where barrier reefs are absent, the unrestricted tidal flow allows the formation of a large marine sand belt (Ball, 1967; Hine, 1977; Rankey and Reeder, 2011; Sparks and Rankey, 2013)

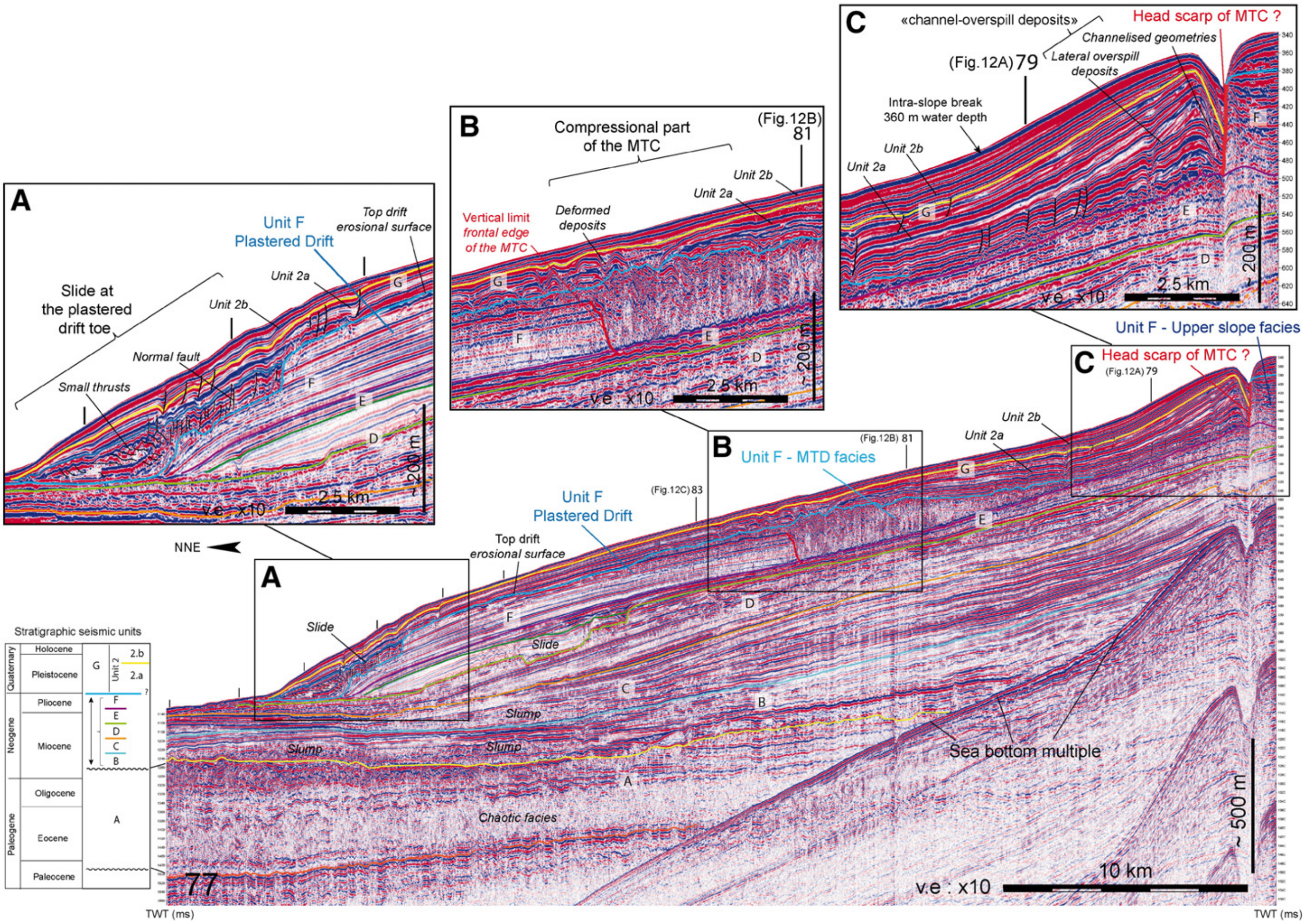

Fig. 11. Seismic features of the frontally confined Mass Transport Complex (MTC) occurring within the plastered drift (HR seismic dip line 77; see location in Fig. 9). Seven seismic stratigraphic units (numbered from A to G) have been identified on line 77. Seismic Unit F is mainly composed of plastered drift that onlap the unconformity surface (top E) and downlap onto the lower slope. Zoom A shows evidence of destabilisations at the toe of the drift, with small thrusts and normal faults. The upper part of Unit F is marked by a chaotic facies, interpreted as reflecting Mass Transport Deposits (MTDs). Zoom B illustrates the frontal edge and the confined character of MTC within the plastered drift. The potential head scarp of MTC is the upslope escarpment (zoom C), underlined by the red line, that forms a circular scarp on the seafloor. Finally, Unit G partially fills the landslide depressions. Within this unit, both channelised geometries and lateral overspill deposits (zoom C) suggest the implication of bottom currents during the filling.

(Figs. 2 and 9). This margin morphology combined with the westward oriented winds induced an increase of the off-bank transport, observed along the leeward open margin of the LBB western corner (Hine and Neumann, 1977; Hine et al., 1981a). Along the slope, the off-bank sediments are remobilised by the Florida and Antilles currents, which leads to accretion of this part of the slope (Hine et al., 1981a,b). Consequently the western corner of the LBB slope can be considered to result from the interplay between (1) off-bank transport (2) and bottom current sedimentation, these two processes being controlled by climate-driven eustatic sea-level changes and global tectonics. This sedimentary framework controls the overall development of the wide slide and downslope destabilizations (3), along the northern slope of LBB (Fig. 16).

(1) The off-bank transport is apparently controlled by seasonal and global climatic–eustatic fluctuations. Some authors identified an off-bank sediment transport during storms and not during normal tidal-current fluctuations (Hine et al., 1981a). Others stated that off-bank sand transport by normal tidal currents and wave action is minor, but their conditions are sufficient to allow the export of carbonate platform mud to the slope (Pilskaln et al., 1989). In addition, Wilson and Roberts (1992, 1995) identified density cascading along the Bahamian bank margin. This process is triggered during winter cold front conditions and leads to the acceleration of the off-bank transport of shallow-water mud (Wilson and Roberts, 1992, 1995). Betzler et al. (2014) showed that sedimentation along the GBB slope is controlled by hyperpycnal flows and contour currents which formed a sedimentary body which they called a periplatform drift. On a large temporal scale, the platform-derived sedimentation is controlled by variations in the global eustatic sea level. Droxler and Schlager (1985) and Schlager et al. (1994) showed that the off-bank transport is more important during highstands in sea level, when the shallow-water carbonate platform is flooded and sediment productivity is maximal.

(2) The bottom current sedimentation is also controlled by climatic–eustatic fluctuations. Temperature and salinity variations modify the intensity of oceanic currents as a response to the associated major change in the thermohaline circulation. However, the North Atlantic oceanic circulation is also influenced by the geodynamic context *e.g.*, final closure of the Isthmus of Panama at 3.5 Ma (Coates et al., 1992) which induced an intensification of the deep ocean circulation (Haug and Tiedemann, 1998; Haug et al., 2001).

(3) Several mechanisms can initiate submarine landslides, such as earthquakes, diapirism, large storms, high sedimentation rates

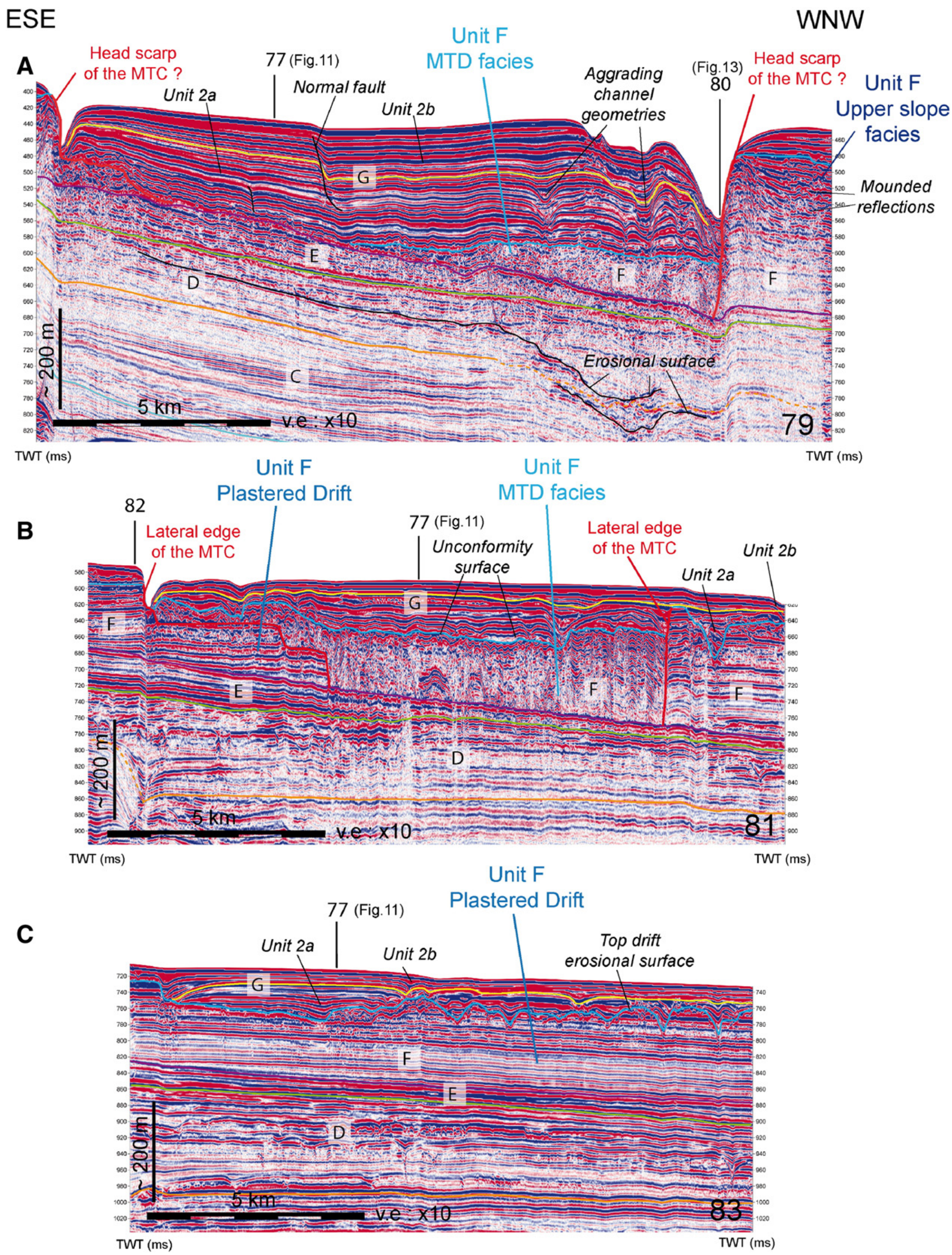

Fig. 12. Seismic illustration of the lateral confinement of the MTC (HR seismic strike lines 79, 81 and 83; see location in Fig. 9). The lateral edge of this MTC forms a circular vertical edge on the present day seafloor. Within Unit G (line 79), normal faults, small slides and aggrading channel (can be interpreted as ancient buried pockmarks) suggest the unstable nature of this filling unit.

or high internal pore pressures (Frey-Martínez et al., 2011; Hampton et al., 1996; Laberg and Vorren, 2000; Locat and Lee, 2002). In this study high sedimentation rates are proposed to be the dominating factor generating sediment overloading. However, this mechanism does not have to be the sole condition for slope failure (Frey-Martínez et al., 2011) as the triggering of submarine landslides could be favoured by an intensification of bottom currents or by a seismic activity.

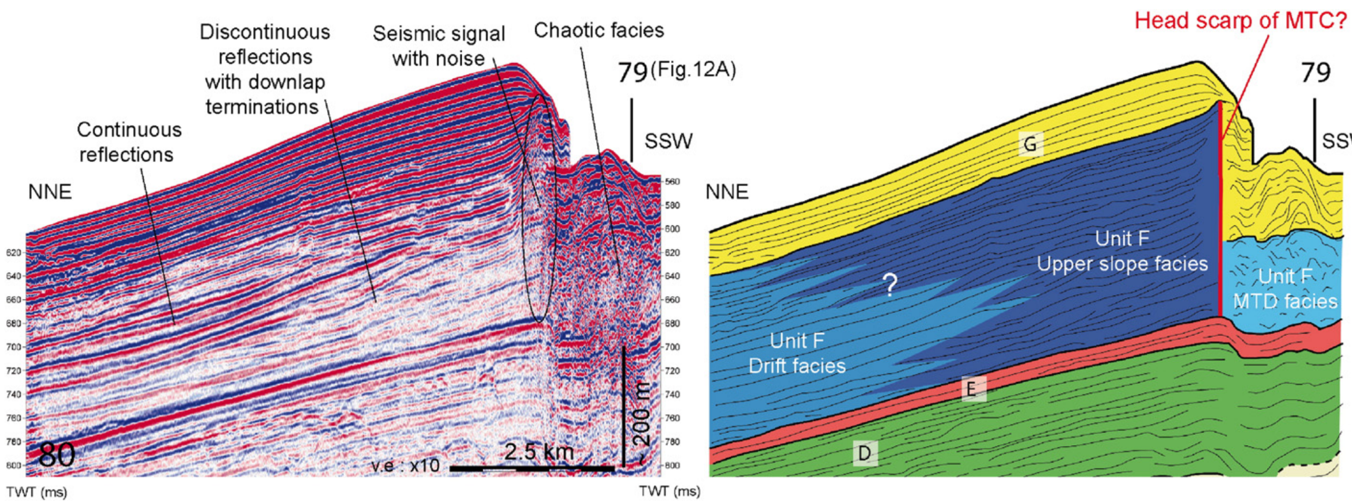

Fig. 13. HR seismic short dip line 80 (located in Fig. 9), illustrating the interplay between the upper slope sediments and the sediment drift with the interfingering of the low-amplitude discontinuous seismic facies with downlap terminations and continuous reflections.

In our study, break out zones of the wide slide have been identified within the upper part of Unit F and its top is marked, in its distal part, by a major erosional surface (Fig. 14). The link between submarine slides and a major erosional surface suggests that the triggering of slides is due to an increase in bottom current circulation (dated roughly during the Pliocene). The study area is mainly influenced by the SE-NW flowing Antilles Current, which may have induced a lateral shift of sediments on the northern slope of the Bahamas. Chérubin (2014)

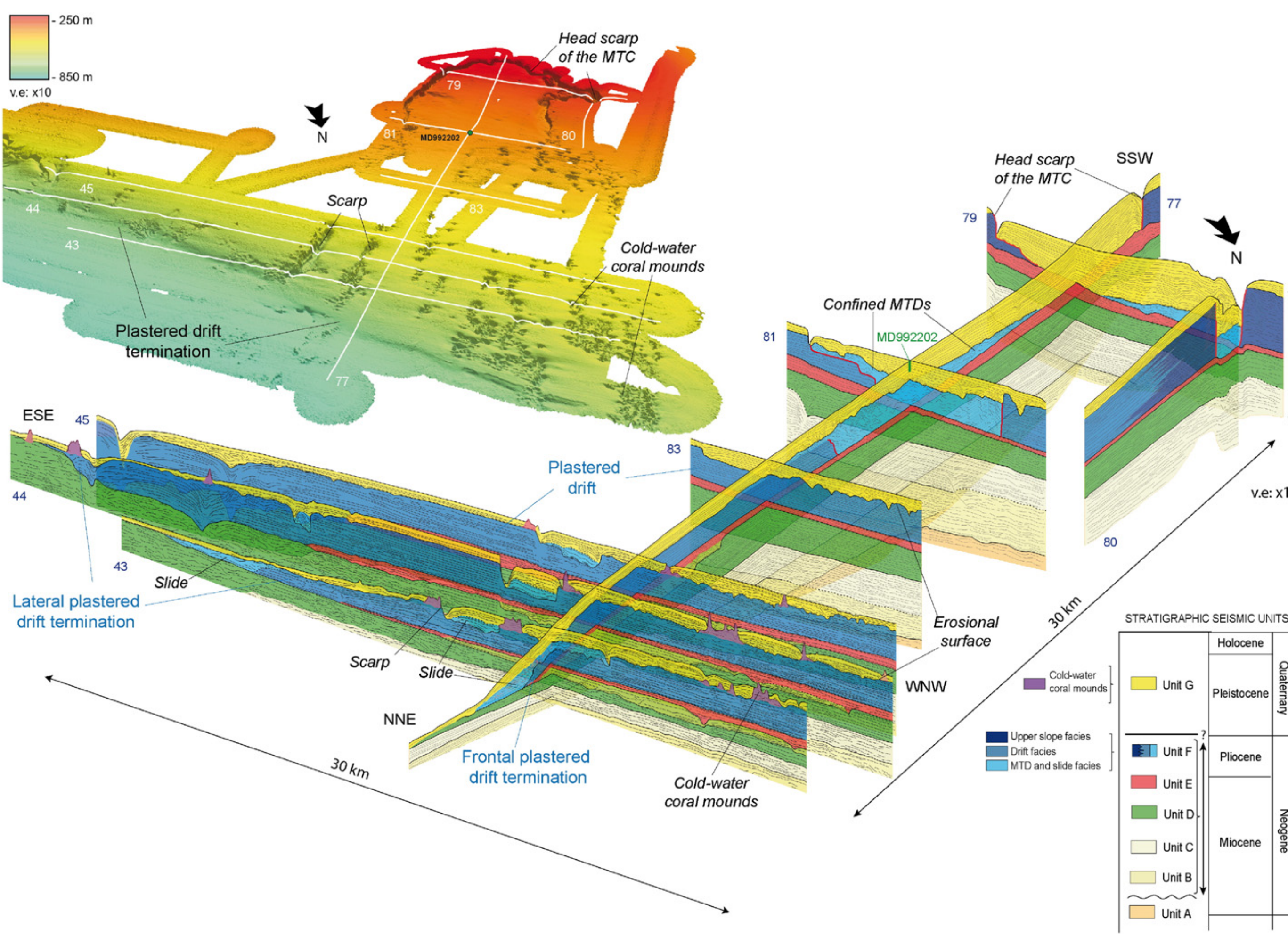

Fig. 14. Fence diagram of the HR seismic line interpretations illustrating the large-scale architecture of the confined MTC, delimited by vertical frontal and lateral edges. The circular vertical edge seen on the seafloor is thought to correspond to the head scarp of the MTC.

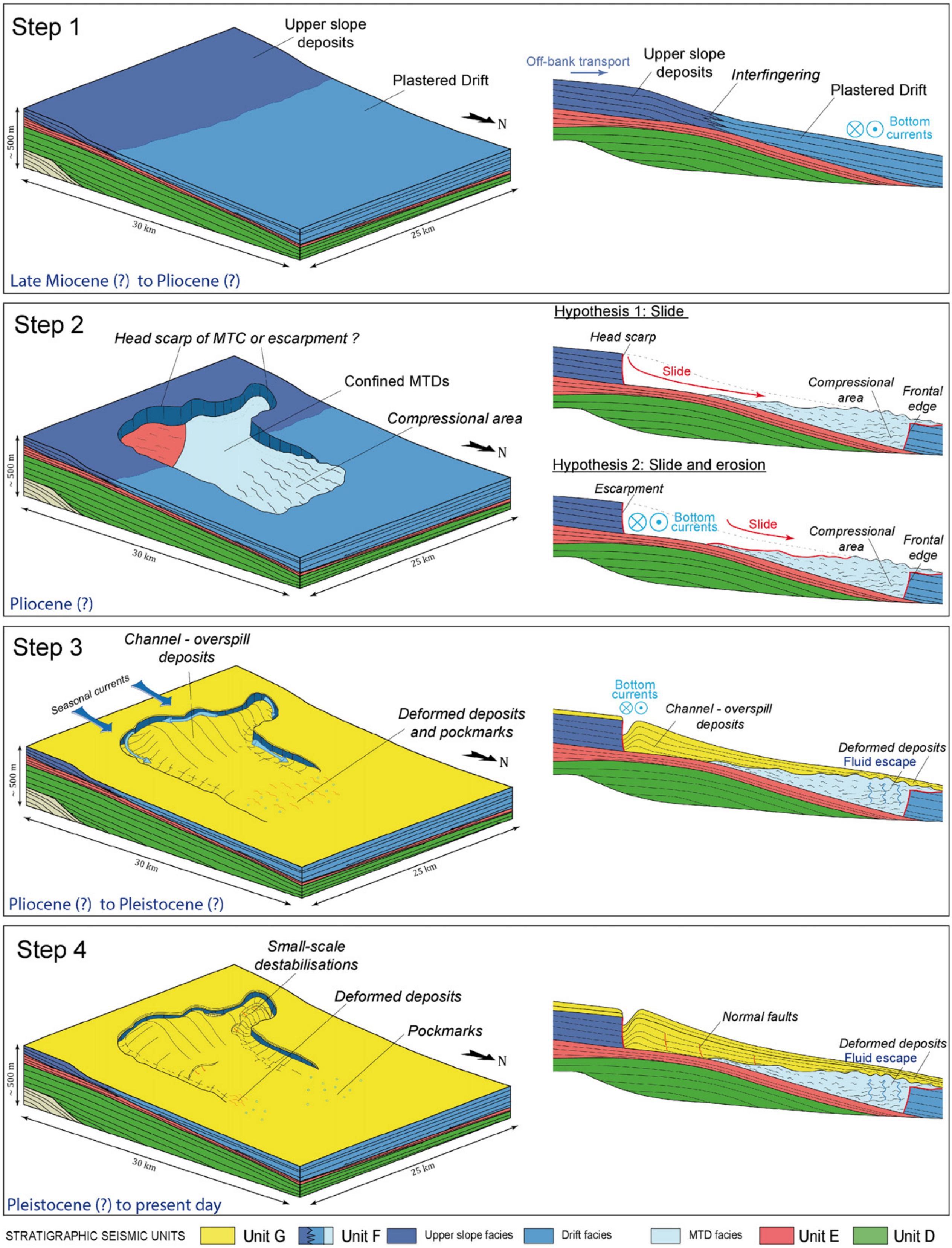

Fig. 15. Schematic diagrams and simplified sections illustrating the MTC formation and evolution on the upper part of Unit F. The drift sediments are interfingered with the sediments coming from the platform (step 1). Step 2 corresponds to the initiation of the frontally confined MTC within the plastered drift. Their formation could be only the result of submarine landslides (hypothesis 1 — step 2), but the absence of MTDs against the scarp potentially suggests the implication of bottom currents which would have eroded the MTDs (hypothesis 2 — step 2). Step 3 corresponds to the filling of the topographic depressions. This filling unit is affected by the motion of the underlying MTDs, where fluid escapes induce pockmarks. Finally, the periplatform ooze sediments cover all the previous units and form the present day seafloor; they are affected by small-scale failures and normal faults that suggest an unstable state of the filling unit (step 4).

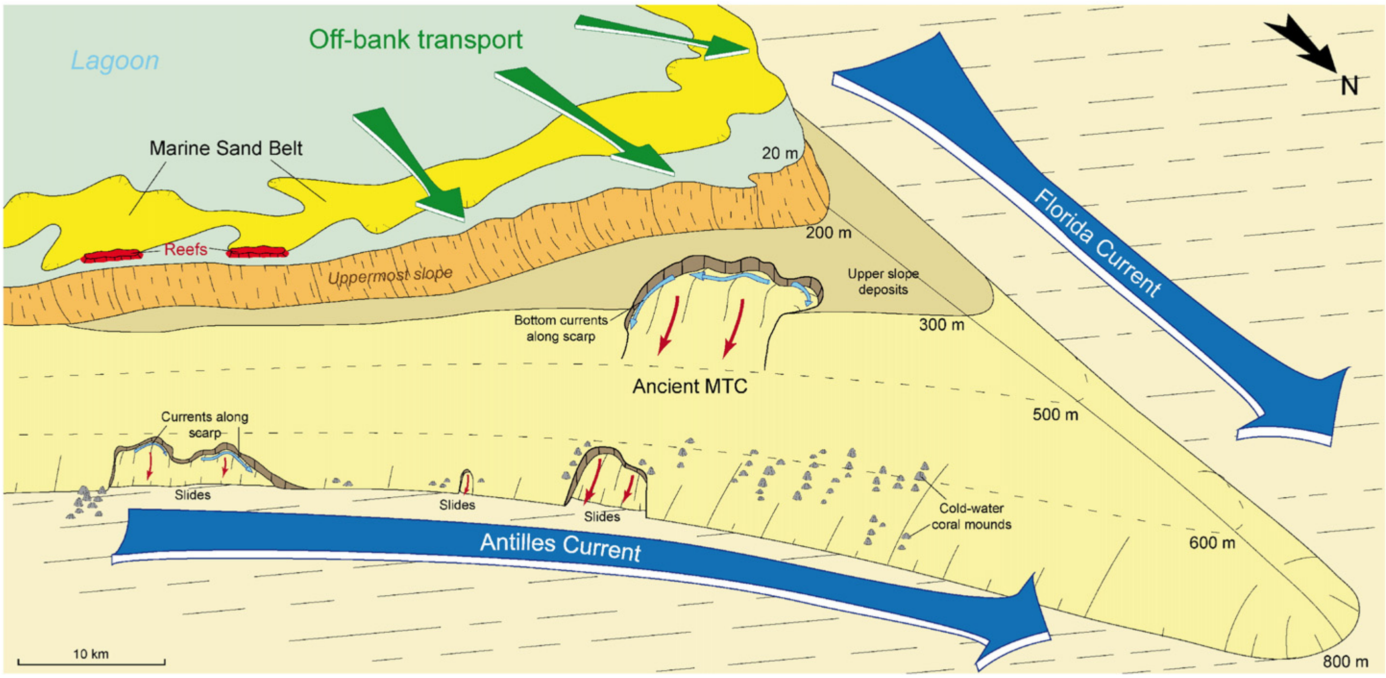

Fig. 16. Summary sketch of the sedimentary dynamics of the LBB northwest corner, driven by the interactions between off-bank transport, bottom current sedimentation and submarine landslides. This extentional growth slope is driven by the off-bank sediment transport associated with the deep-sea bank-derived sediments influenced by the combined action of the Florida and Antilles currents. Add to the ancient MTC observed between 275 m and 460 m water depths, the downslope failures at the toe of plastered drift are present between 650 m and 800 m water depths. Along the same bathymetrical interval, the cold-water mounds are distributed near the slides.

estimated northern transport flow velocities within the uppermost water column, above 1000 m water depth, to vary between 5 Sv (2005 value) and 27 Sv (2007 value) in winter and early spring.

Seismic activity could be another triggering mechanism. Previous studies have shown the effect of the Walker Cay Faults that run perpendicular to the adjacent bank margin, which offset late Oligocene deposits by as much as 100 m (Mullins and Mark Van Buren, 1981; Van Buren and Mullins, 1983). However, although these faults induce a complex Late Oligocene paleogeography, they do not seem to have affected the Neogene sediments of the northwest slope of LBB.

Finally, submarine landslides could be favoured by the presence of cemented surfaces generated by early diagenesis behaving as a preferential detachment horizon and gliding plane for the slided sediments. The northern LBB slope is marked by numerous detachment surfaces in the Pliocene–Holocene interval, which control large-scale rotational movements and slumped masses (Harwood and Towers, 1988).

5.4. Comparison with other MTCs

The recent high-resolution survey, multibeam bathymetry and seismic profiles, along the western slope of GBB enables the detailed characterisation of the slope failures (Jo, 2013; Mulder et al., 2012a). The dataset collected during Carambar Leg 1 (Mulder et al., 2012a; Principaud et al., 2015-in this issue) reveals three failure scarps, at 650 m water depth, extending in a north–south direction over 9 km, related to large rectangular blocks downstream. Principaud et al. (2015-in this issue) demonstrate that these MTCs are not connected to any drift destabilisation, unlike the northwest corner of the LBB slope. High sedimentation rates were identified as the main triggering factor. For the slope failures observed further south, Jo (2013) and Jo et al. (2015-in this issue) proposed that a seismic shock could be an additional triggering parameter. In the southern domain of the GBB slopes the Santaren Anticline forms the northward frontal termination of the Cuba–Bahamas collision. Deformation processes were still active during the late Paleogene, the Neogene and probably also the Quaternary (Masaferro and Eberli, 1999).

Several submarine landslides were also detected along the US Atlantic continental slope (McAdoo et al., 2000; Twichell et al., 2009). These submarine landslides affected the continental shelf-edge in the continuity of the Blake Escarpment. These large slope failures (maximum width of 15–30 km) are mainly driven by earthquakes associated with the isostatic rebound of the glaciated part of the margin or earthquakes associated with salt domes (Twichell et al., 2009).

The direct comparison between the Mass Transport Deposits of our study with ancient outcropping MTDs remains difficult because the 3D continuity of outcrops is rarely large enough to represent the large scale of MTDs. However, geometrical comparisons can be performed through seismic-based studies of ancient offshore systems. Many examples of MTDs are described in the offshore context (McAdoo et al., 2000; Moscardelli and Wood, 2008; Shipp et al., 2011). Among them, the submarine landslide of the Thebe complex (Scarselli et al., 2013), along the Exmouth Plateau in the Northwest shelf of Australia, represented an excellent analog of the LBB slope in terms of scale and geometry. Although the inferred triggering mechanisms are different from those of our study, the size of the slide is similar with a length of at least 20 km, a lateral extension of at least 12 km, and a thickness between 50 m and 200 m. Moreover, this submarine slide is also frontally confined and the frontal ramp marks the downdip transition to a series of extensional slide blocks and an outer thrust belt (Scarselli et al., 2013).

6. Conclusions

This study proposes an integrated and multi-scale analysis of a new example of carbonate MTC along the Bahamian slopes, which occurs at the northwest corner of the LBB slope. Sedimentary patterns appear to be driven by the complex interaction between significant off-bank transport and deep-water reworking of bank-derived sediments by the combined action of the Florida and Antilles currents.

The originality of this case study lies in the unusual meandering character of the MTC scarp, still visible on the sea bottom. The detailed and comprehensive understanding of the internal architecture of this MTC has been performed through the interpretation of HR seismic lines. This detailed analysis revealed that the MTC is composed of confined MTDs, developed within the upper section of a plastered drift, approximately of Pliocene age.

The compressional part of the MTC induces fluid circulation, which occurred in the frontal part of the large submarine slide. This process is evidenced by the formation of numerous pockmarks visible on the sea floor. Moreover, the downslope movement of the deposits overlying the MTC, expressed by several small-scale slope failures and normal faults, suggests the unstable character of the Quaternary deposits that ultimately could be at the origin of new mass wasting events, which would then create a composite stack of amalgamated MTCs.

Despite these new understandings, a confident determination of the potential trigger(s) of this MTC remains contentious. However, it may be envisaged that the studied MTC is linked to a major erosional surface occurring at the top of the plastered drift in its distal part. This observation suggests that a period of intensification of bottom current activity played a major role in the initiation of the MTC. This study emphasises the diversity and complexity of the sedimentary processes controlling the shape and depositional processes on Bahamian carbonate slopes, and therefore provides new insights to improve the understanding of the spatial and temporal evolution of carbonate slopes.

Acknowledgements

We thank the captain and the crew of the *R/V Le Suroît* for the quality of the data acquired during the Carambar cruise 1. We acknowledge TOTAL for their support and their scientific contribution to this project. The authors are grateful to reviewers Gregor Eberli and Xavier Janson for their constructive comments and suggestions which significantly improved the early version of this manuscript. Editor John Reijmer is also warmly thanked, not only for his technical contribution but also for his significant help concerning the written English of the text. Finally, the authors also wish to thank Samuel Etienne for his thoughtful comments and significant input on the manuscript.

References

Anselmetti, F.S., Eberli, G.P., Ding, Z.-D., 2000. From the Great Bahama Bank into the Straits of Florida: a margin architecture controlled by sea-level fluctuations and ocean currents. Geological Society of America Bulletin 112, 829–844.

Austin, J.A., Schlager, W., Palmer, A.A., Comet, P.A., Droxler, A., Eberli, G.P., Fourcade, E., Freeman-Lynde, R., Fulthorpe, C.S., Harwood, G., Kuhn, G., Lavoie, D., Leckie, M., Melillo, A.J., Moore, A., Mullins, H.T., Ravenne, C., Sager, W.W., Swart, P., Verbeek, J.W., Watkins, D.K., Williams, C., 1986. Proceedings of the Ocean Drilling Program, Initial Reports Leg. 101.

Ball, M.M., 1967. Carbonate sand bodies of Florida and the Bahamas. Journal of Sedimentary Research 37, 556–591.

Bergman, K.L., 2005. Seismic Analysis of Paleocurrent Features in the Florida Straits: Insights into the Paleo-Florida Current, Upstream Tectonics, and the Atlantic–Caribbean Connection. University of Miami, (206 pp.).

Bergman, K., Westphal, H., Janson, X., Poiriez, A., Eberli, G., 2010. Controlling parameters on facies geometries of the Bahamas, an isolated carbonate platform environment. In: Westphal, H., Riegl, B., Eberli, G.P. (Eds.), Carbonate Depositional Systems: Assessing Dimensions and Controlling Parameters. Springer, Netherlands, pp. 5–80.

Betzler, C., Reijmer, J.J.G., Bernet, K., Eberli, G.P., Anselmetti, F.S., 1999. Sedimentary patterns and geometries of the Bahamian outer carbonate ramp (Miocene–Lower Pliocene, Great Bahama Bank). Sedimentology 46, 1127–1143.

Betzler, C., Lindhorst, S., Eberli, G.P., Lüdmann, T., Möbius, J.r, Ludwig, J., Schutter, I., Wunsch, M., Reijmer, J.J.G., Hübscher, C., 2014. Periplatform drift: the combined result of contour current and off-bank transport along carbonate platforms. Geology 42 (10), 871–874.

Borgomano, J.R.F., 2000. The Upper Cretaceous carbonates of the Gargano–Murge region, Southern Italy: a model of platform-to-basin transition. AAPG Bulletin 84, 1561–1588.

Chérubin, L.M., 2014. High-resolution simulation of the circulation in the Bahamas and Turks and Caicos Archipelagos. Progress in Oceanography.

Coates, A.G., Jackson, J.B.C., Collins, L.S., Cronin, T.M., Dowsett, H.J., Bybell, L.M., Jung, P., Obando, J.A., 1992. Closure of the Isthmus of Panama: the near-shore marine record of Costa Rica and western Panama. Geological Society of America Bulletin 104, 814–828.

Correa, T.B.S., Grasmueck, M., Eberli, G.P., Reed, J.K., Verwer, K., Purkis, S.A.M., 2012. Variability of cold-water coral mounds in a high sediment input and tidal current regime, Straits of Florida. Sedimentology 59, 1278–1304.

Crevello, P.D., Schlager, W., 1980. Carbonate debris sheets and turbidites, Exuma Sound, Bahamas. Journal of Sedimentary Research 50, 1121–1147.

Damuth, J.E., 1980. Use of high-frequency (3.5–12 kHz) echograms in the study of near-bottom sedimentation processes in the deep-sea: a review. Marine Geology 38, 51–75.

Droxler, A.W., Schlager, W., 1985. Glacial *versus* interglacial sedimentation rates and turbidite frequency in the Bahamas. Geology 13, 799–802.

Eberli, G.P., Ginsburg, R.N., 1989. Cenozoic progradation of northwestern Great Bahama Bank, a record of lateral platform growth and sea-level fluctuations. In: Crevello, J.L., Wilson, J.L., Sarg, J.F., Read, J.F. (Eds.), Controls on Carbonate Platforms and Basin Development. SEPM (Society for Sedimentary Geology) Special, Publication 44, pp. 339–351.

Eberli, G.P., Swart, P.K., McNeill, D.F., Kenter, J.A.M., Anselmetti, F.S., Melim, L.A., Ginsburg, R.N., 1997. A synopsis of the Bahamas Drilling Project: results from two deep core borings drilled on the Great Bahama Bank. In: Eberli, G.P., Swart, P.K., Malone, et al. (Eds.), Proceedings of the Ocean Drilling Program, Initial Reports, Leg 166: College Station, Texas, Ocean Drilling Program.

Faugères, J.-C., Stow, D.A.V., Imbert, P., Viana, A., 1999. Seismic features diagnostic of contourite drifts. Marine Geology 162, 1–38.

Frey-Martínez, J., Cartwright, J., James, D., 2006. Frontally confined *versus* frontally emergent submarine landslides: a 3D seismic characterisation. Marine and Petroleum Geology 23, 585–604.

Frey-Martínez, J., Bertoni, C., Gérard, J., Matías, H., 2011. Processes of submarine slope failure and fluid migration on the Ebro continental margin: implications for offshore exploration and development. In: Shipp, R.G., Weimer, P., Posamentier, H.R. (Eds.), Mass-transport Deposits in Deepwater Settings. SEPM (Society for Sedimentary Geology) Special Publication 96, pp. 181–198.

Ginsburg, R.N., Harris, P.M., Eberli, G.P., Swart, P.K., 1991. The growth potential of a bypass margin, Great Bahama Bank. Journal of Sedimentary Research 61, 976–987.

Hampton, M.A., Lee, H.J., Locat, J., 1996. Submarine landslides. Reviews of Geophysics 34, 33–59.

Harwood, G.M., Towers, P.A., 1988. Seismic sedimentological interpretation of a carbonate slope, north margin of Little Bahama Bank. In: Austin, J.A., Schlager, W., Palmer, A.A., et al. (Eds.), Proceedings of the Ocean Drilling Program, Scientific Results, Leg. 101, pp. 263–277.

Haug, G.H., Tiedemann, R., 1998. Effect of the formation of the Isthmus of Panama on Atlantic Ocean thermohaline circulation. Nature 393, 673–676.

Haug, G.H., Tiedemann, R., Zahn, R., Ravelo, A.C., 2001. Role of Panama uplift on oceanic freshwater balance. Geology 29, 207–210.

Hine, A.C., 1977. Lily Bank, Bahamas; history of an active oolite sand shoal. Journal of Sedimentary Research 47, 1554–1581.

Hine, A.C., Neumann, A.C., 1977. Shallow carbonate-bank-margin growth and structure, Little Bahama Bank, Bahamas. AAPG Bulletin 61, 376–406.

Hine, A.C., Wilber, R.J., Bane, J.M., Neumann, A.C., Lorenson, K.R., 1981a. Offbank transport of carbonate sands along open, leeward bank margins: Northern Bahamas. Marine Geology 42, 327–348.

Hine, A.C., Wilber, R.J., Neumann, A.C., 1981b. Carbonate sand bodies along contrasting shallow bank margins facing open seaways in northern Bahamas. AAPG Bulletin 65, 261–290.

Janson, X., Kerans, C., Loucks, R., Marhx, M.A., Reyes, C., Murguia, F., 2011. Seismic architecture of a Lower Cretaceous platform-to-slope system, Santa Agueda and Poza Rica fields, Mexico. AAPG Bulletin 95, 105–146.

Jo, A., 2013. Carbonate slope morphology and sedimentary processes along southwestern Great Bahama Bank. Thesis Master of Science (MS), Marine Geology and Geophysics. University of Miami (102 pp.).

Jo, A., Eberli, G.P., Grasmueck, M., 2015. Margin collapse and slope failure along southwestern Great Bahama Bank. Sedimentary Geology 317, 43–52 (in this issue).

Laberg, J.S., Vorren, T.O., 2000. The Trænadjupet Slide, offshore Norway — morphology, evacuation and triggering mechanisms. Marine Geology 171, 95–114.

Lantzsch, H., Roth, S., Reijmer, J.J.G., Kinkel, H., 2007. Sea-level related resedimentation processes on the northern slope of Little Bahama Bank (Middle Pleistocene to Holocene). Sedimentology 54, 1307–1322.

Locat, J., Lee, H.J., 2002. Submarine landslides: advances and challenges. Canadian Geotechnical Journal 39, 193–212.

Masaferro, J.L., Eberli, G.P., 1999. Jurassic–Cenozoic structural evolution of the southern Great Bahama Bank. In: Mann, P. (Ed.), Caribbean Basins: Sedimentary Basins of the World. 4, pp. 167–193.

McAdoo, B.G., Pratson, L.F., Orange, D.L., 2000. Submarine landslide geomorphology, US continental slope. Marine Geology 169, 103–136.

Moscardelli, L., Wood, L., 2008. New classification system for mass transport complexes in offshore Trinidad. Basin Research 20, 73–98.

Mulder, T., Ducassou, E., Eberli, G.P., Hanquiez, V., Gonthier, E., Kindler, P., Principaud, M., Fournier, F., Léonide, P., Billeaud, I., Marsset, B., Reijmer, J.J.G., Bondu, C., Joussiaume, R., Pakiades, M., 2012a. New insights into the morphology and sedimentary processes along the western slope of Great Bahama Bank. Geology 40, 603–606.

Mulder, T., Ducassou, E., Gillet, H., Hanquiez, V., Tournadour, E., Combes, J., Eberli, G.P., Kindler, P., Gonthier, E., Conesa, G., Robin, C., Sianipar, R., Reijmer, J.J.G., François, A., 2012b. Canyon morphology on a modern carbonate slope of the Bahamas: evidence of a regional tectonic tilting. Geology.

Mullins, H.T., Cook, H.E., 1986. Carbonate apron models: alternatives to the submarine fan model for paleoenvironmental analysis and hydrocarbon exploration. Sedimentary Geology 48, 37–79.

Mullins, H.T., Hine, A.C., 1989. Scalloped bank margins: beginning of the end for carbonate platforms? Geology 17, 30–33.

Mullins, H., Mark Van Buren, H., 1981. Walkers Cay Fault, Bahamas: evidence for Cenozoic faulting. Geo-Marine Letters 1, 225–231.

Mullins, H.T., Neumann, A.C., 1979. Deep carbonate bank margin structure and sedimentation in the northern Bahamas. In: Doyle, L.J., Pilkey, O.H. (Eds.), Geology of Continental Slopes. SEPM (Society for Sedimentary Geology) Special Publication 27, pp. 165–192.

Mullins, H.T., Boardman, M.R., Neumann, A.C., 1979. Echo character of off-platform carbonates. Marine Geology 32, 251–268.

Mullins, H.T., Neumann, A.C., Wilber, R.J., Hine, A.C., Chinburg, S.J., 1980. Carbonate sediment drifts in northern Straits of Florida. AAPG Bulletin 64, 1701–1717.

Mullins, H.T., Heath, K.C., Van Buren, H.M., Newton, C.R., 1984. Anatomy of a modern open-ocean carbonate slope: northern Little Bahama Bank. Sedimentology 31, 141–168.

Mullins, H.T., Gardulski, A.F., Wise, S.W., Applegate, J., 1987. Middle Miocene oceanographic event in the eastern Gulf of Mexico: implications for seismic stratigraphic succession and loop current/Gulf Stream circulation. Geological Society of America Bulletin 98, 702–713.

Phelps, R.M., Kerans, C., 2007. Architectural characterization and three-dimensional modeling of a carbonate channel–levee complex: Permian San Andres Formation, Last Chance Canyon, New Mexico, U.S.A. Journal of Sedimentary Research 77, 939–964.

Pilskaln, C.H., Neumann, A.C., Bane, J.M., 1989. Periplatform carbonate flux in the northern Bahamas. Deep Sea Research Part A. Oceanographic Research Papers 36, 1391–1406.

Playton, T., Janson, X., Kerans, C., 2010. Carbonates slopes. In: James, N.P., Dalrymple, R.W. (Eds.), Facies Models 4, Geological Association of Canada, pp. 449–476.

Principaud, M., Mulder, T., Gillet, H., Borgomano, J., 2015. Large-scale carbonate submarine mass-wasting along the northwestern slope of the Great Bahama Bank (Bahamas): Morphology, architecture, and mechanisms. Sedimentary Geology 317, 27–42 (in this issue).

Rankey, E.C., Doolittle, D.F., 2012. Geomorphology of carbonate platform–marginal uppermost slopes: insights from a Holocene Analogue, Little Bahama Bank, Bahamas. Sedimentology 7, 2146–2171.

Rankey, E.C., Reeder, S.L., 2011. Holocene oolitic marine sand complexes of the Bahamas. Journal of Sedimentary Research 81, 97–117.

Reeder, S.L., Rankey, E.C., 2008. Interactions between tidal flows and ooid shoals, Northern Bahamas. Journal of Sedimentary Research 78, 175–186.

Reeder, S.L., Rankey, E.C., 2009. Controls on morphology and sedimentology of carbonate tidal deltas, Abacos, Bahamas. Marine Geology 267, 141–155.

Reijmer, J., Betzler, C., Kroon, D., Tiedemann, R., Eberli, G., 2002. Bahamian carbonate platform development in response to sea-level changes and the closure of the Isthmus of Panama. International Journal of Earth Sciences 91, 482–489.

Richardson, P.L., 1983. Gulf Stream rings. In: Robinson, A. (Ed.), Eddies in Marine Science, Topics in Atmospheric and Oceanographic Sciences. Springer, Berlin Heidelberg, pp. 19–45.

Richardson, P.L., Cheney, R.E., Worthington, L.V., 1978. A census of Gulf Stream rings, spring 1975. Journal of Geophysical Research, Oceans 83, 6136–6144.

Savary, B., Ferry, S., 2004. Geometry and petrophysical parameters of a calcarenitic turbidite lobe (Barremian-Aptian, Pas-de-la-Cluse, France). Sedimentary Geology 168, 281–304.

Scarselli, N., McClay, K., Elders, C., 2013. Submarine slide and slump complexes, Exmouth Plateau, NW Shelf of Australia. In: Keep, M., Moss, S.J. (Eds.), The Sedimentary Basins of Western Australia IV: Proceedings of the Petroleum Exploration Society of Australia Symposium, Perth, WA.

Schlager, W., Ginsburg, R.N., 1981. Bahama carbonate platforms — the deep and the past. Marine Geology 44, 1–24.

Schlager, W., James, N.P., 1978. Low-magnesian calcite limestones forming at the deep-sea floor, Tongue of the Ocean, Bahamas. Sedimentology 25, 675–702.

Schlager, W., Reijmer, J.J.G., Droxler, A., 1994. Highstand shedding of carbonate platforms. Journal of Sedimentary Research 64, 270–281.

Schlee, J.S., Dillon, W.P., Grow, J.A., 1979. Structure of the continental slope off the eastern United States. In: Doyle, L.J., Pilkey, O.H. (Eds.), Geology of Continental Slopes. SEPM (Society for Sedimentary Geology) Special Publication 27, pp. 95–117.

Sheridan, R.E., Drake, C.L., Nafe, J.E., Hennion, J., 1966. Seismic-refraction study of continental margin east of Florida. AAPG Bulletin 50, 1972–1991.

Sheridan, R.E., Gradstein, F.M., Barnard, L.A., Bliefnick, D.M., Habib, D., Jenden, P.D., Kagami, H., Keenan, E.M., Kostecki, Kvenvolden, K.A., Moullade, M., Ogg, J., Robertson, A.H.F., Roth, P.H., Shipley, 1983. Initial Reports of the Deep Sea Drilling Project Leg. 76.

Shipp, R.G., Weimer, P., Posamentier, H.R., 2011. Mass-transport deposits in deepwater settings. SEPM (Society for Sedimentary Geology) Special Publication 96 (527 pp.).

Sparks, A.G., Rankey, E.C., 2013. Relations between geomorphic form and sedimentologic–stratigraphic variability: Holocene ooid sand shoal, Lily Bank, Bahamas. AAPG Bulletin 97, 61–85.

Steph, S., Tiedemann, R., Prange, M., Groeneveld, J., Nürnberg, D., Reuning, L., Schulz, M., Haug, G.H., 2006. Changes in Caribbean surface hydrography during the Pliocene shoaling of the Central American Seaway. Paleoceanography 21, PA4221.

Twichell, D.C., Chaytor, J.D., ten Brink, U.S., Buczkowski, B., 2009. Morphology of late Quaternary submarine landslides along the U.S. Atlantic continental margin. Marine Geology 264, 4–15.

Van Buren, H.M., Mullins, H.T., 1983. Seismic stratigraphy and geologic development of an open-ocean carbonate slope; the northern margin of Little Bahama Bank. In: Sheridan, R.E., Gradstein, F.M., Barnard, L.A., et al. (Eds.), Initial Reports of the Deep Sea Drilling Project Leg 76. U.S. Govt. Printing Office, Washington, pp. 749–762.

Vecsei, A., Sanders, D.G.K., 1997. Sea-level highstand and lowstand shedding related to shelf margin aggradation and emersion, Upper Eocene–Oligocene of Maiella carbonate platform, Italy. Sedimentary Geology 112, 219–234.

Weimer, P., 1989. Sequence stratigraphy of the Mississippi fan (Plio-Pleistocene), Gulf of Mexico. Geo-Marine Letters 9, 185–272.

Wilson, P.A., Roberts, H.H., 1992. Carbonate-periplatform sedimentation by density flows: a mechanism for rapid off-bank and vertical transport of shallow-water fines. Geology 20, 713–716.

Wilson, P.A., Roberts, H.H., 1995. Density cascading; off-shelf sediment transport, evidence and implications, Bahama Banks. Journal of Sedimentary Research 65, 45–56.